Packaging Technology and Science

WILEY

Packaging Technology and Science
An International Journal

RESEARCH ARTICLE OPEN ACCESS

Functionality and Storage Evaluation of Fish Freshness Indicators Based on the Incorporation of Anthocyanins Extracted From Winery Grape Pomace Into Polyvinyl Alcohol/Starch Films

Evgenia Basdeki[1] | Enrico Maurizzi[2] | Franscesco Bigi[3] | Andrea Quartieri[3] | Andrea Pulvirenti[2] | Theofania Tsironi[1]

[1]Laboratory of Food Process Engineering, Department of Food Science and Human Nutrition, Agricultural University of Athens, Athens, Greece | [2]Department of Life Sciences, University of Modena and Reggio Emilia, Modena, Italy | [3]Packtin, Reggio Emilia, Italy

Correspondence: Theofania Tsironi (ftsironi@aua.gr)

Received: 24 April 2025 | **Revised:** 3 June 2025 | **Accepted:** 11 June 2025

Funding: This work was supported by Horizon 2020 Framework Programme (872217) and Hellenic Foundation for Research and Innovation (20599).

Keywords: anthocyanins | film storage | fish | shelf life | smart labels | vineyard pomace

ABSTRACT

Novel smart packaging systems demonstrate great potential in addressing challenges related to cold chain management and in reducing food waste. This study focused on the development of smart indicators composed of polyvinyl alcohol and starch, infused with anthocyanins extracted from winery residues. The extract held an adequate amount of anthocyanins (~339 mg/L cyanidin-3-glucoside equivalents) and showed increased pH sensitivity. Similarly, the obtained smart indicators exhibited high pH responsivity ($\Delta E = 39.37$) and exhibited sensitivity to volatile amines, as tested with trimethylamine (ΔE reached 53.34), dimethylamine (ΔE reached 54.71) and ammonia vapour solutions (ΔE reached 57.69). Based on microstructure and infrared spectra, the incorporation of anthocyanins slightly enhanced the miscibility of the polymers. Water solubility, swelling index and wettability values did not show significant variations between the control indicators and the smart indicators. The films were also evaluated for water adsorption, water solubility, wettability and colour stability over a 45-day storage period under three different temperatures (5°C, 15°C and 25°C) and five distinct relative humidity (33%, 56%, 75%, 90% and 98%) environments. Increased temperature and relative humidity conditions compromised the functional properties of the films. Subsequently, the smart indicators were incorporated into sealed packages of gilthead sea bream to monitor fish freshness under constant and variable temperature conditions. Fish spoilage was verified using microbiological (total viable counts, *Pseudomonas* spp. and Enterobacteriaceae) as well as physicochemical (pH, total volatile basic nitrogen) indices. The colour change (from pinkish-red to pale green-blue) of the smart indicators, along with the total colour difference (ΔE reached 23.5 at constant and 35.7 at variable temperature conditions), indicated that the fabricated smart labels were capable of reflecting temperature fluctuations during fish storage and providing insights into the spoilage level of the packaged fish.

1 | Introduction

The global challenge of increasing food demand and waste is well documented in the literature [1, 2]. Fish and seafood are commodities that are also experiencing this trend worldwide, characterized by a rising volume of waste [3]. This can be attributed to their perishable nature; consequently, fish and seafood undergo significant biochemical changes after harvest,

resulting in a noticeable deterioration in quality and considerable financial losses. Waste is spotted at several levels of the fish supply chain, including the distribution, retail and consumer stages [4]. Smart freshness labels represent a valuable solution for reducing waste at both the household and retail stages, offering consumers an intuitive and accessible means to visually assess the freshness of fish [5, 6].

Significant advancements have been achieved in packaging-related research regarding the development of smart films that monitor the deterioration of food product quality and contribute to shelf life prediction [7, 8]. Materials derived from petroleum contribute to environmental pollution due to their slow and challenging degradation, resulting in their accumulation in both terrestrial and marine environments [9]. With the introduction of increasing regulations on packaging sustainability (EU Regulation 2025/40), which mandate the restriction of excess packaging, the pursuit of biodegradable and environmentally friendly packaging materials presents a significant challenge [10]. Several attempts have been made towards the introduction of more sustainable materials in the food packaging sector [11–13]. Biopolymers, that is, starch, chitosan, polyvinyl alcohol (PVA), gelatin and methylcellulose, serve as effective alternatives to synthetic plastics due to their solubility in water, biodegradability and exceptional film-forming properties. To enhance the structural integrity and stability of the films, various biopolymer combinations have been investigated for the development of smart films, with the compatibility of the polymers playing a crucial role. Starch is favoured for its biodegradability and film-forming capacities; however, it often demonstrates brittleness and high sensitivity to moisture. Nevertheless, blending it with chitosan is recognized to enhance its stability and reduce its water uptake [14]. Similarly, starch-based films exhibit significant improvements in flexibility and mechanical resistance with the incorporation of PVA into the film, as PVA functions as a plasticizer and promotes intermolecular interactions [12, 13]. The incorporation of reinforcing agents, such as chitin whiskers and bentonite nanoclays, further enhances the strength of the films and reduces their water vapour permeability [14, 15].

The use of natural pigments as pH-sensitive compounds that change colour throughout the fish shelf life is becoming increasingly attractive due to the disadvantages associated with synthetic dyes, such as toxicity [16]. The most common natural pigments include anthocyanins [17], betalains [6] and curcumin [18]. Several researchers have investigated the fabrication of smart packaging solutions based on PVA and starch, incorporating anthocyanins into their formulation [16, 17]. In their study, Zhai et al. [19] examined the addition of roselle anthocyanins to PVA/starch films and observed enhanced compatibility between the two polymers, as well as an overall improvement in the functionality of the smart films due to the incorporation of anthocyanins. Similar findings were reported by Liu et al. [20] for PVA/starch films containing purple sweet potato.

The utilization of anthocyanins extracted from agricultural waste enhances the sustainability of the final indicators and positively contributes to the principles of circular economy. Typical examples of agricultural by-products include plum and prune residues of berries [21], black rice bran, purple sweet potato peels, red cabbage outer leaves [22] and pomegranate leftovers from juice extraction [23]. Grape pomace, a widely recognized waste material from the winemaking industry, is both economical and environmentally friendly due to its abundance and high content of bioactive compounds, making it a viable alternative to synthetic dyes. The use of such industrial by-products not only reduces waste but also complies with circular economy regulations, further promoting the transition towards sustainable food packaging technology.

Despite the increased potential of smart freshness indicators in reducing food waste by visually revealing the product's state of freshness, there are limitations regarding the large-scale application of smart labels [24]. Some of these include the stability of the pH-sensitive compounds when the surrounding temperature and humidity conditions fluctuate as well as the interaction of the smart packaging materials with the moisture inside the food package headspace [25]. These aspects that highly affect the indicators longevity are intensified when biopolymers and water-soluble materials in general are involved in the development of the smart packaging systems [26]. Also, the detection precision and sensitivity of the freshness indicators may vary, creating a need for standardized production methods of the freshness indicators [25].

Film storage conditions represent a significantly less researched parameter in literature. Environmental factors such as temperature, relative humidity (RH) and light may influence the stability of both polymer matrix and the pH-sensitive pigment. High levels of humidity can cause the premature degradation or dissolution of water-soluble films, whereas temperature fluctuations may result in the pigments changing colour at a rate that exceeds the rate of accurate colour response. Zhai et al. [19] studied the colour stability of smart PVA/starch/anthocyanin films conditioned for 14 days at 4°C and 25°C under 75% RH and concluded that colour was retained adequately at both temperatures; however, better colour sensitivity results were reported for films kept at 4°C. The self-stability of the colourimetric films was essential to their final colour performance, due to the fact that smart films interacted with oxygen and were partially oxidized as storage time increased. The overall colour change of the smart films stored at 25°C was around 4%–5%, whereas the colour change of the films stored at 4°C was $< 1\%$, highlighting the effect of temperature on the functionality of the anthocyanins.

Romruen et al. [27] investigated the effect of temperature and RH on smart films based on sodium alginate/butterfly pea anthocyanins/catechin–lysozyme agar containing cellulose nanospheres. According to their results, increased RH conditions seemed to compromise the integrity of the films, probably due to the excessive interaction of water molecules with the structural units of the polymers. Conversely, temperature emerged as a more significant factor influencing colour stability, with improved colour retention observed at 4°C. An interesting finding was that after cellulose nanospheres incorporation in the film matrix, the colour stability of the films increased (lower colour change during storage) regardless of storage temperature or humidity level. Cellulose nanospheres may have acted as a barrier against oxidative factors

(i.e., oxygen and light) and moisture due to their hydrophobic nature, thus protecting anthocyanin from degradation. These findings highlight the necessity of investigating the reliability and longevity of smart freshness films prior to their actual implementation, particularly for indicators designed to monitor the freshness of food products, such as fish, where the humidity levels of the packaging headspace tend to increase (e.g., 90% RH).

In this context, the present study focused on the development of pH-sensitive freshness labels based on PVA and starch, infused with anthocyanins derived from winery grape pomace. By integrating biopolymers and natural pigments, this study aims to provide an environmentally sustainable approach to monitor fish spoilage while simultaneously valourizing agricultural waste. Additionally, the study aims to investigate various storage scenarios of smart films to highlight the significance of temperature and RH on the integrity and functionality of the films. The main advantages of the proposed freshness indicators compared to other relevant smart packaging systems are based on the utilization of vineyard pomace to extract anthocyanins, thus promoting the circular economy model. Furthermore, in comparison to other relevant studies, in this work, the smart indicators were tested simultaneously under multiple RH and temperature conditions for a comparatively longer duration. To provide a more realistic smart packaging solution, the fabricated smart labels were tested for fish shelf life monitoring under constant and variable temperature conditions, simulating potential temperature fluctuations in the actual cold chain.

2 | Materials and Methods

2.1 | Materials

Packtin s.r.l. (Reggio Emilia, Italy) provided dried winery grape pomace, recovered as winemaking residue from wine production in Reggio Emilia, Italy. PVA with a molecular weight of 27 kDa and a 98% degree of hydrolysis was purchased from Fluka (Steinheim, Germany). Starch powder was purchased from Merck (Darmstadt, Germany). Disodium phosphate, citric acid, glycerol (≥ 99.5%), hydrochloric acid solution, trimethylamine (TMA), dimethylamine (DMA) and ammonia (NH_3) solutions were provided by Sigma-Aldrich (St. Louis, MO, USA). Plate count agar (PCA), cetrimide agar (CFC) and violet red bile glucose agar (VRBG) used for microbial enumeration were purchased from Condalab (Torrejon De Ardoz, Spain). Ringer tablets were purchased from Merck (Darmstadt, Germany). The gilthead seabream (*Sparus aurata*) fillets used for the shelf life test were obtained from AVRAMAR SA (Greece).

2.2 | Anthocyanin Extraction

Dried and milled grape pomace (comprising grape skins, seeds and pulp) was used as a raw material to extract anthocyanins using the solvent-based extraction method described by Alizadeh Sani et al. [28]. The pomace powder was blended with 80/20 (v/v) distilled water/ethanol at a plant material-to-solvent ratio of 1:20 (w/v). Mild stirring followed (24 h at 25°C ± 2°C, in the dark) and then mixtures were filtered through Whatman Grade 4 filter paper (Whatman plc—Cytiva) × 5 times and centrifuged at 5000 × g for 10 min at 4°C. Anthocyanins were concentrated through a rotary evaporator with vacuum pump (37°C, 25 mmHg).

2.3 | Anthocyanin Characterization

2.3.1 | Determination of Total Anthocyanin Content

pH differential technique (AOAC Official Method 2005.02) was used to evaluate the total anthocyanin content of the pomace extract through spectrophotometry at 520 and 700 nm. The pH differential method essentially calculated the amount of anthocyanin present in the sample by measuring the absorbance (A) of the sample at two different pH values (1.0 and 4.5) at the same wavelength λvis-max (520 nm) with a spectrophotometer. The difference in the absorbance of the samples at λvis-max (520 nm) was proportional to the concentration of the pigment. The absorbance measurement at 700 nm was conducted to correct for haze/turbidity. Total monomeric anthocyanin content (expressed as cyanidin-3-glucoside equivalents) was calculated using Equation (1):

$$\text{Anthocyanin pigment (cyanidin} - 3 - \text{glucoside equivalents, mg/L)} = \frac{A \, x \, MW \, x \, DF \, x \, 1000}{\varepsilon \, x \, l} \quad (1)$$

where A = (absorbance at 520 nm–absorbance at 700 nm) at pH 1.0 minus (absorbance at 520 nm–absorbance at 700 nm) at pH 4.5, MW = molecular weight of the predominant anthocyanin (cyanidin-3-glucoside, 449.2 g/mol), DF = dilution factor, ε = molar absorptivity (26 900 L/mol·cm for cyanidin-3-glucoside) and l = path length of the cuvette (usually 1 cm).

2.3.2 | Anthocyanin pH Responsivity

Buffer solutions were prepared across a pH range of 2–12 by mixing a disodium hydrogen phosphate solution (0.2 M) with a citric acid solution (0.1 M) at appropriate ratios. The pH-dependent colour-changing ability of the anthocyanins was assessed by dissolving the anthocyanins in the pH 2–12 buffer solutions and recording their colour (CIE L*, a* and b*) using a colour spectrophotometer (i1Pro, X-Rite) [29].

2.4 | Preparation of Smart Labels

Control and smart films were produced through the solvent casting method. Starch and PVA were dissolved by stirring in distilled water at 90°C for 60 min, and glycerol (10% w/w of dry matter) was added as plasticizer. Smart labels were prepared by incorporating the anthocyanin-rich extract (0.37% v/v) in the aqueous solution of starch (4% w/v): PVA (2% w/v) at a 3:1 ratio [27, 28]. 0.5 mL HCl (37%) was added to the final film-forming solutions to stabilize anthocyanins. Following the complete dissolution of the dry mass, 20 mL of the film-forming solution were cast into clean Petri dishes and placed

in an incubator at 40°C for 24 h to dry under dark conditions. The films were subsequently peeled from the Petri dishes and stored at 50% RH for further use [30].

2.5 | Characterization of Smart Labels

2.5.1 | Thickness and Optical Properties

Film thickness was measured with a digital micrometer (IP65, SAMA Tools, Viareggio, Lucca, Italy) at 10 different randomly chosen positions. The average and standard deviation of 10 measurements were recorded. The analysis of optical properties included the colour measurement of the films (CIE L*, a* and b*) using a colour spectrophotometer (i1 PRO, x rite), as well as the evaluation of light barrier properties, measured using a spectrophotometer (VWR Douple Beam UV × Vis 6300 PC spectrophotometer, China). The light transmittance of the films was assessed in the visible wavelength range (380–730 nm) [31].

2.5.2 | pH Responsivity of Smart Labels

A pH-responsivity test was conducted to evaluate the pH-dependent colour changing ability of the smart labels [32]. Buffer solutions were prepared at a range of pH values from 2 to 12, as described in Section 2.3.2, and were gently applied on the surface of the smart labels for the evaluation of the colour response. The colour response was measured using a colour spectrophotometer and expressed through the colour parameters L (lightness, black = 0 to white = 100), a (greenness = −60 to redness = +60) and b (blueness = −60 to yellowness = +60). The determination of the total colour difference (ΔE) was calculated using Equation (2):

$$\Delta E = \sqrt{(L - L_O)^2 + (a - \alpha_O)^2 + (b - b_O)^2} \quad (2)$$

where L_0, a_0 and b_0 represent the initial values of the colour parameters and L, a and b denote the values recorded after the pH response test.

2.5.3 | Sensitivity to Volatile Amines

Smart labels were evaluated for the ability to detect volatile amines commonly produced during fish spoilage, such as TMA, DMA and NH_3 vapour, according to the method described by Kuswandi et al. [33] with slight modifications. The smart labels were positioned 1 cm above a flask containing an aqueous solution (20 mL) of TMA, DMA and NH_3, each tested separately at various concentrations (0.002–1 M) for maximum duration of 20 min to evaluate the sensitivity of the labels. The flasks containing the smart labels on top were placed inside larger sealed containers (~50 mL in volume) during the sensitivity test to prevent the leakage of the volatilized compounds and to generate an 'isolated headspace', simulating a fish package. The colour parameters L, a and b were measured using a colour spectrophotometer, and the total colour difference (ΔE) was calculated according to Equation (2).

2.5.4 | Scanning Electron Microscopy

Scanning electron microscopy (SEM) was used to analyse the microstructure of the cast films using an Everhart–Thornley detector (ETD) in combination with HiVac mode that allows the detection of secondary electrons and provides images of ultra high resolution. Surface and cross-section micrographs were observed at 5000× and 1000× magnification, respectively, for all cast films.

2.5.5 | Fourier Transform Infrared Spectroscopy (FT-IR)

An FT-IR spectrometer was used to measure the infrared spectra (Alpha, Bruker Optik GmbH, Ettlingen, Germany) of the films in the wavenumber range of 4000–600 cm^{-1} with 64 scans at a resolution of 4 cm^{-1}. Three replicates of each spectrum were captured.

2.5.6 | Moisture Content (MC), Water Solubility (WS) and Swelling Index (SI)

The moisture content (MC) of the films was determined gravimetrically by measuring the weight loss of the films (cut at 1 × 5 cm^2) before (W_1) and after (W_2) drying at 105°C for 24 h. Five replicates of each film were evaluated. The MC value was calculated using Equation (3):

$$\mathrm{MC} = \frac{W1 - W2}{W1} \mathrm{x}\, 100 \quad (3)$$

For the determination of WS and SI, films were cut into 1 × 5 cm pieces and left to dry in a desiccator with dried silica for 7 days. Once the films were completely dry, they were weighed (W_3). According to the method suggested by Oliveira et al. [34], the dry films were immediately immersed in containers with 20 mL of distilled water, where they were left to soak for 24 h.

After removal from the water, the films were softly blotted on tissue paper to remove residual water and weighed again (W_4). SI was calculated using Equation (4):

$$\mathrm{SI} = \frac{W4 - W3}{W3} \times 100\,\% \quad (4)$$

For the determination of WS, the films were dried at 105°C for 24 h and subsequently weighed until a constant weight was achieved (W_5). Five replicates of each film were evaluated. Total soluble matter (TSM) was calculated using Equation (5):

$$\mathrm{TSM}\,\% = \frac{W3 - W5}{W3} \times 100\,\% \quad (5)$$

2.5.7 | Wettability

Static contact angle measurement was performed using the sessile drop method with a Theta Flow Optical Tensiometer (Biolin Scientific, Gothenburg, Sweden) according to ASTM D5946 method. The films were adhered to glass slides, and a droplet of deionized water (4 μL) was placed on the surface of each film.

The sessile drop technique was performed at room temperature in ambient air. The determination of the static contact angle, 'θ', at the three-phase line of contact relied on fitting of the drop profile, often using the Young–Laplace equation [35]. The mean contact angle was measured from 3 different film replicates and on 5 points on the surface of each film (for a total of 15 replicates) by analysing the shape of the droplet using OneAttension software.

2.6 | Storage of Smart Labels

2.6.1 | Conditioning of Films at Various Temperature and Humidity Conditions

Considering that the smart labels produced in this research are intended for use in environments with high RH (such as fish packaging) and are distributed through cold chain systems, it is important to investigate the effect of different storage conditions on the final properties of the films [27]. Therefore, control and smart films were conditioned under three different storage temperatures (5°C, 15°C and 25°C) and five distinct RH environments (RH 33%, 56%, 75%, 90% and 98%). Most research studies to date have been testing the effect of storage temperature of films at 4°C and 25°C [19, 27, 36]. Therefore, based on the lack of an intermediate temperature, 15°C was chosen to be investigated in the current study. More specifically, dry films (1 × 5 cm) with five replicates were placed in weighing bottles and stored inside five glass desiccators, each containing a specific saturated salt solution selected to create constant and specific RH within the desiccator. The salts used were $MgCl_2$, $Mg(NO_3)_2$, NaCl, $BaCl_2$ and K_2SO_4. Each set of five desiccators was placed inside three high-precision (±0.2°C) low-temperature incubators (Sanyo MIR 153, Sanyo Electric, Ora-Gun, Gunma, Japan) set at 5°C, 15°C and 25°C. Equilibrium was achieved after 15 days, at which point the initial measurements were taken. The storage of the films continued for a total of 45 days, with measurements described below conducted every 15 days.

2.6.2 | Adsorption Isotherms

Adsorption isotherms were employed to express the amount of water absorbed by the samples, in each storage scenario. The equilibrium moisture (g water/g dry base) of the samples was determined as described below. The water was analysed as being divided into two components: the first layer (monolayer) and the remaining layers, which were assumed to have uniform properties (multilayer). Monolayer moisture (M_0) is a critical parameter of moisture sorption, as it indicates the point at which all available binding sites for water molecules are occupied. GAB equation (6) was used to fit the experimental data, and the parameters of the equation were determined as described by Blahovec and Gianniotis [37]. The properties of the remaining layers were different from the monolayer and were represented by the parameter k of GAB equation (6).

$$X = \frac{M_O \; C \; a_w}{(1 - a_w)\;(1 - k \; a_w + C \; k \; a_w)} \tag{6}$$

where X is the moisture (g water/g dry base) of the film, a_w is the water activity, M_0 is the monolayer moisture of the film on a dry basis and C, k are dimensionless parameters.

2.6.3 | Colour and Light Barrier Properties of Films During Storage

All films stored under different temperature and RH conditions were analysed for colour (CIE L*, a* and b*) and light barrier properties as described in Section 2.5.1 at different time intervals (15, 30 and 45 days). Light absorbance of the films was measured in the visible wavelength range (380–730 nm).

2.6.4 | WS of Films During Storage

TSM % of all films stored under different temperature and RH conditions was determined as described in Section 2.5.6 at different time intervals (15, 30 and 45 days).

2.6.5 | Wettability of Films During Storage

Static contact angle measurement of all films stored under various conditions was performed by the sessile drop method using Theta Flow Optical Tensiometer (Biolin Scientific, Gothenburg, Sweden) according to ASTM D5946 method, as described in Section 2.5.7.

2.7 | Fish Freshness Monitoring

To validate the functionality of the fabricated smart labels, a shelf life monitoring experiment was conducted on fresh gilthead sea bream (*S. aurata*) fillets. After cutting the smart films into dimensions of 2 × 2 cm two replicates were attached inside sterilized packaging pouches (polyethylene/polyamide low-permeability pouches, 70 μm thick and measuring 15 × 20 cm). 50 g of fresh gilthead sea bream fillets were also placed inside the pouches, which were then sealed and stored for shelf life monitoring. All measurements were carried out at appropriate time intervals during fish storage.

2.7.1 | Storage of Fish Under Constant and Variable Temperature Conditions

Fish freshness monitoring was conducted under various storage conditions (both more and less favourable conditions to fish spoilage) to evaluate the sensitivity of the smart labels in detecting different rates of fish spoilage. Therefore, fresh gilthead sea bream filets were stored under constant (1.7°C) and variable temperature conditions (ranging from 1.3°C to 25.6°C and set randomly). Temperature in the incubators was constantly monitored with electronic, programmable miniature dataloggers (RC-5 USB Temperature Data Logger Recorder, Elitech Ltd, UK). Fish quality level was determined using the Arrhenius-based kinetics developed from the data obtained from the isothermal experiments. To demonstrate the integrated effect of temperature variability on product quality,

the term effective temperature (T_{eff}) was introduced. Effective temperature equals a constant temperature that resulted in the same quality value as the variable temperature distribution over the same period [38].

2.7.2 | Microbial Growth Measurement

The microbiological aspects of fish spoilage were determined throughout the shelf life experiment [39]. Fish skin and flesh (10 g) were diluted with 90-mL sterilized Ringer solution into a sterile bag using a Stomacher device (BagMixer, Interscience, Saint-Nom-la-Breteche, France) for 90 s. For microbial enumeration, a volume of 0.1-mL sample homogenate of 10-fold serial dilutions was spread on the surface of appropriate growth media in Petri dishes. For total viable count (TVC) enumeration, the plates (plate count agar) were incubated at 25°C for 72 h, whereas for *Pseudomonas* spp., plates (cetrimide agar) were incubated at 25°C for 48 h. For Enterobacteriaceae enumeration, the pour plate method (violet red bile glucose agar) was used with incubation at 25°C for 48 h. Sampling for microbiological analysis was performed on experiment days 0, 1, 2, 5, 7 and 9. Microbial load was expressed as the average log cfu/g. Two replicates of three appropriate dilutions were enumerated per fish sample and spoilage microorganism.

2.7.3 | pH and TVB-N Content

Physiochemical quality markers, such as pH and total volatile basic nitrogen (TVB-N), were determined during the storage of fish fillets under all tested storage conditions.

pH of the homogenized fish samples (10 g of fish flesh at 90-mL Ringer solution) was measured at room temperature at appropriate time intervals using the edge HI2002 pH meter, equipped with digital glass body pH electrode (Hanna Instruments Inc.).

TVB-N content was determined using Conway's microdiffusion method. 4 g fish flesh sample were added to 16 mL of 4% w/v trichloroacetic acid and homogenized with Ultra Turrax T25 basic (IKA-Werke GmbH & Co.), repeatedly at room temperature. The sample extract was then filtered through Whatman Grade 4 filter paper (Whatman plc—Cytiva). One millilitre of the obtained supernatant was placed in the outer ring of the Conway apparatus, and 1 mL of the inner ring solution (1% boric acid containing the Conway indicator) was placed into the inner ring of the apparatus. Finally, 1 mL of saturated K_2CO_3 solution was mixed with the sample extract. The Conway apparatus was sealed, manually shaken and incubated at 37°C for 60 min. The inner ring solution was then titrated with 0.02 N HCl using a microburette until the green colour turned to pink. TVB-N content was calculated using Equation (7):

$$\text{TVB}-\text{N (mg/100 g fish)} = (V_s - V_b)\ (N_{HCl}\, A_N)\, \frac{\left[\left(W_s\ \frac{M}{100}\right) + V_E\right] 100}{W_s} \quad (7)$$

where V_S is the titration volume of 0.02 N HCl for sample extract (mL), V_B is the titration volume for blank (mL), N_{HCl} is the normality of HCl, A_N is the atomic weight of nitrogen, W_S is the weight of muscle sample (g), M is the percentage moisture of muscle sample and V_E is the volume of 4% TCA used in extraction (mL).

2.7.4 | In-Package Gas Composition

The in-package gas composition was measured using a gas analyser (Danseonsor, CheckPoint 3) at all sampling points of the fish storage experiment.

2.7.5 | Colour Response of Smart Labels

Colour evaluation of the smart labels was conducted at all sampling points of the fish shelf life experiment to assess their ability to respond to fish quality alterations. Colour parameters (CIE L*, a* and b*) were monitored at each time interval with a colour spectrophotometer (i1PRo X-Rite). Total colour difference (ΔE) and change in colour parameter a, Δa ($a_{initial}$–a_{final}) of the smart labels were monitored as described in Section 2.5.2 and calculated according to Equation (2).

2.8 | Statistical Analysis

The data obtained during the experimental processes were fitted using the Baranyi Growth Model and curve fitting was enabled through DMfit 3.5 software (IFR, Institute of Food Research, Reading, UK) (available at http://www.combase.cc/index.php/en/, accessed on 20 January 2025). Significant differences for the parameters studied were determined using Duncan's multiple range test at a significance level of 95% (a = 0.05).

3 | Results and Discussion

3.1 | Anthocyanin Characterization

3.1.1 | Total Anthocyanin Content

Total anthocyanin content of the extract was ~339 mg/L cyanidin-3-glucoside equivalents.

3.1.2 | Anthocyanin pH Responsivity

The pH of the anthocyanins extract was measured and was equal to 3.36. The colour variations of anthocyanins in response to pH levels are attributed to their structural transformations in different buffer solutions. Table 1 presents the change of the colour parameters L, a and b as well as images of the extract during exposure to various pH buffer solutions. At acidic pH levels from 1 to 3, anthocyanins predominantly exist in the form of flavylium cations, which impart red colouration. As the pH increases to 4–7, the molecular structure transitions to that of the colourless carbinol pseudobase and purple quinonoidal base. In the pH range of 7–8, anthocyanins are converted into their anionic quinonoidal base form, resulting in a blue appearance. At higher alkaline pH levels,

TABLE 1 | Colour parameters and digital images of the anthocyanin extract exposed to pH buffer solutions.

pH	L	a	b	Image
Control	26.96 ± 2.28^{b}	43.87 ± 1.71^{d}	30.84 ± 2.34^{e}	
2	27.90 ± 2.16^{b}	45.53 ± 2.32^{d}	34.93 ± 2.12^{e}	
5	41.86 ± 1.36^{d}	19.37 ± 0.36^{c}	11.96 ± 0.91^{d}	
6	31.59 ± 1.89^{bc}	17.71 ± 2.04^{c}	8.28 ± 0.74^{c}	
7	25.85 ± 2.04^{b}	12.51 ± 0.89^{b}	5.72 ± 0.02^{b}	
8	15.64 ± 0.85^{a}	6.40 ± 1.38^{a}	2.43 ± 0.03^{a}	
12	35.01 ± 2.45^{c}	20.78 ± 1.53^{c}	43.58 ± 1.89^{f}	

Note: Data are expressed as mean ± standard deviation. Values with different superscripts in the same column (a–f) indicate statistically significant difference, as determined by Duncan's multiple range test ($p \leq 0.05$).

they convert into the chalcone form, which exhibits a yellow hue [28, 29]. These characteristic colour changes were also observed in anthocyanins extracted from vineyard grapes pomace. Different types of anthocyanins present different colour responses to pH, affected by the plant source [40]. Zhai et al. [19] extracted anthocyanins from roselles and reported slightly different colour change when exposed at pH buffers. Specifically, the colour of anthocyanins solutions was pink at pH lower than 5 and changed gradually to purple at pH 6–7. When the solutions were basic, the colour altered to blue and yellow at pH 8–9 and 10–12, respectively. Luchese et al. [41] monitored the colour change of anthocyanins extracted from blueberry pomace; the colour became red-pink-purple at pH values lower than 5, slightly yellow at pH values 6, 7, 8, 9 and finally brownish and slightly blue in a pH range of 7.0–11.0.

The a-value decreased immediately following exposure to increasing pH levels, with the exception of pH 2. This was anticipated, as the initial pH of the extract was 3.36, thus, exposure to a lower pH resulted in a slight increase. Parameters a and b increased at pH 12, which can be attributed to the orange-yellow colouration associated with the chalcone form of the anthocyanins [42]. Overall, the grape pomace extract appeared to carry a sufficient concentration of anthocyanins and responded appropriately to the various pH buffer solutions.

3.2 | Characterization of Smart Labels

3.2.1 | Thickness and Optical Properties

The average film thickness was 0.1113 ± 0.0107 mm, whereas the control films were slightly thicker with an average thickness of 0.1238 ± 0.0118 mm. However, this difference was not statistically significant.

The PVA/starch smart film incorporating anthocyanins is depicted in Figure 1A. The colour of the film was rose-red, attributed to the inherent colouration of the anthocyanins integrated into the PVA/starch matrix. The measured colour parameters (L, a and b) of the smart labels were 50.11 ± 4.68, 48.87 ± 4.84 and -5.53 ± 0.55, respectively. Comparable findings have been reported by several researchers regarding the colour of smart labels composed of PVA, starch and anthocyanins extracted from various natural sources [16, 43, 44].

Another important optical property assessed was light transmittance, which provided insights into the film's ability to block light (Figure 1B). Transmittance was evaluated within the visible wavelength range (380–730 nm) and exhibited high values for the PVA/starch films (exceeding 65%), particularly beyond 400 nm, indicating the transparency and optical clarity of the control films. This observation was further supported by the colour parameters ($L = 88.03 \pm 1.52$, $a = -0.68 \pm 0.03$ and $b = -5.02 \pm 0.23$), which are characteristic of a colourless and transparent film. The smart labels displayed lower transmittance within the visible wavelength range, possibly due to the incorporation of the extracted anthocyanins that reduced their transparency and provided an intense colouration (an innate characteristic of anthocyanins). There was a sharp reduction in light transmittance of smart labels around 560–580 nm, which is attributed to the absorption spectrum of the anthocyanins, which falls between 450 and 580 nm [45]. A similar decreasing trend in light transmittance, along with a slight increase up to 700 nm, has also been reported in previous studies on anthocyanin-incorporated smart labels [31, 46].

3.2.2 | pH Responsivity of Smart Labels

The fabricated smart labels were exposed to pH buffer solutions ranging from pH 2 to 12 in order to evaluate their pH-dependent colour response. A rapid colour change was observed within

approximately 1 min following the immersion of the labels in each pH buffer solution. The initial colour of the films was characterized by a pinkish-red hue (high a-value and low b-value), as shown in Figure 2. In the acidic pH range (pH 2–4), the a-value remained elevated, although it exhibited a gradual decline. The reddish hue gradually shifted to a more colourless or light purple hue upon exposure to intermediate pH values (5–7), which subsequently transitioned to light green at pH 8–9 and ultimately blue at pH 10–12. Figure 3A illustrates that the a-value, initially measured at 41.93, started to decrease at pH 3, with the rate of decline becoming pronounced until reaching a plateau between pH 7 and 9 (approximately 3), before ultimately decreasing to a lower value of −2.33. In contrast, the b-value, which began at −4.15, exhibited a slower yet visible upward trend as the films were exposed to an increasing pH, with a final value of −0.25. These changes are reflected in the final appearance of the film, which displays a pure blue colour.

Overall, as illustrated in Figure 3B, the total colour difference (ΔE) of the smart labels exceeded 3 and progressively increased with rising pH, ultimately reaching a final ΔE value of 39.37. This indicates that the smart labels were sufficiently responsive

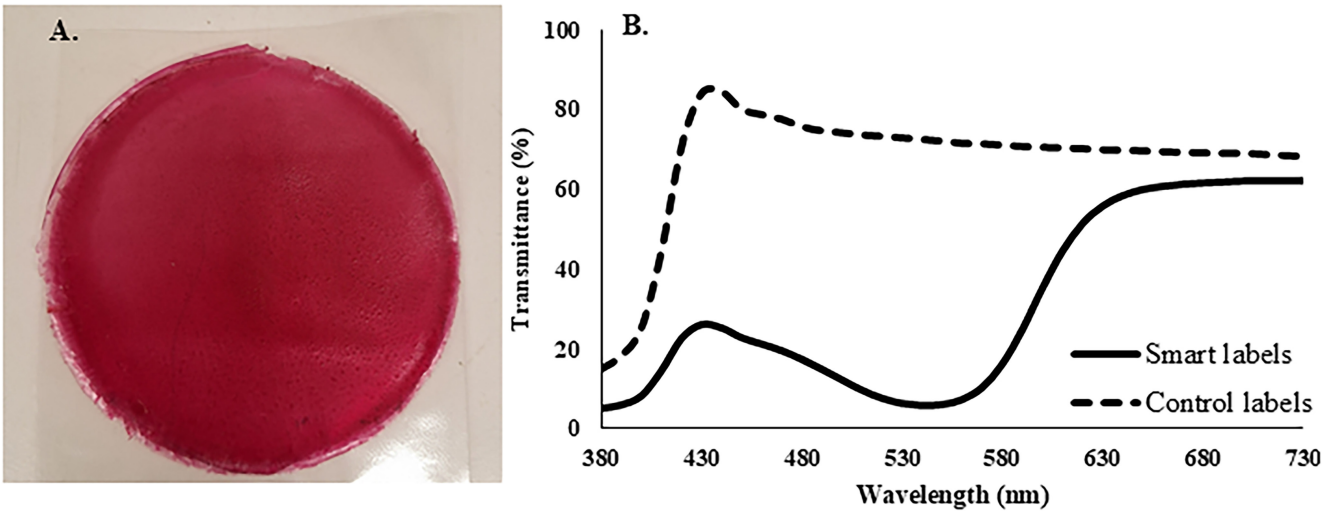

FIGURE 1 | (A) PVA/starch/anthocyanin-based smart label and (B) light transmittance (%) of films with and without the incorporation of anthocyanins.

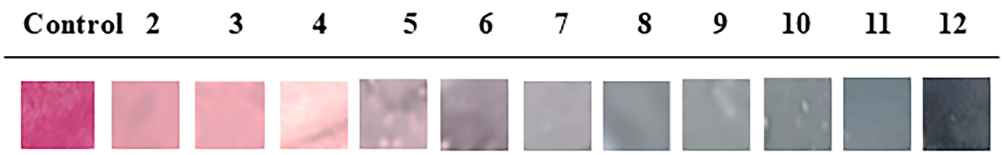

FIGURE 2 | Digital images of the smart labels exposed to pH buffers solutions (2–12).

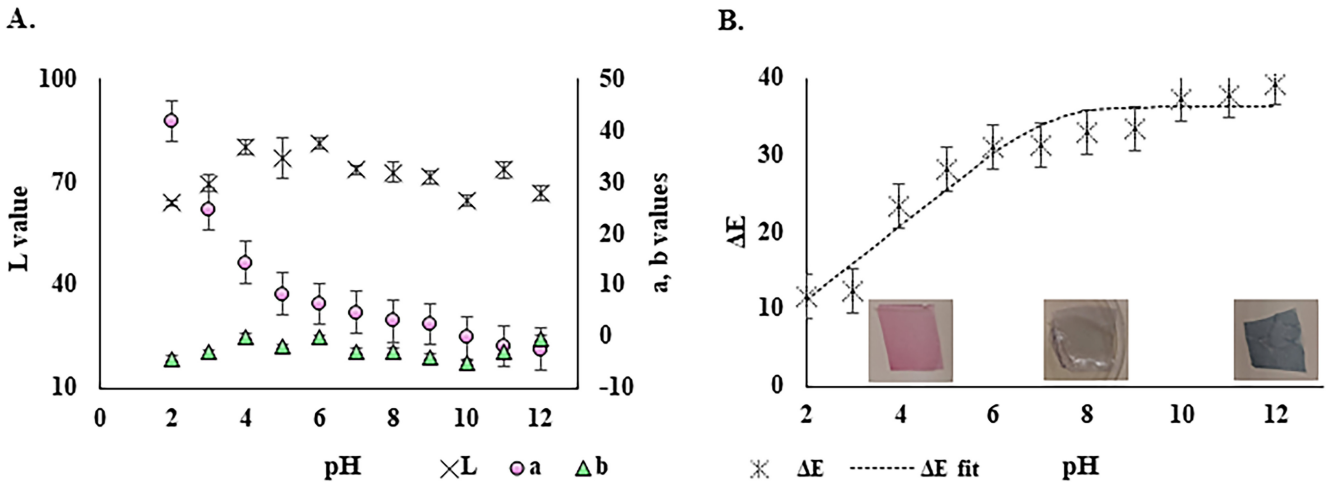

FIGURE 3 | (A) Schematic presentation of the colour parameters L (lightness), a (greenness/redness) and b (yellowness/blueness) and (B) total colour difference (ΔE) after exposure of smart labels to pH 2–12 buffer solutions.

and could provide a clear indication of pH variation. Similar ΔE values have been reported for smart labels based on anthocyanins obtained from other natural sources, such as sweet potato [47] and flowering plants [48].

To further investigate the pH-sensitive properties of the labels following the immobilization of the anthocyanin extract within the PVA/starch matrix, the total colour difference (ΔE) of the labels was compared to the corresponding value of the pure extract. The results, given in Figure 4, indicate that the highest ΔE values were observed when the pure anthocyanin extract was subjected to pH buffer solutions, as anticipated. However, the ΔE values for both the pure extract and the smart labels were relatively close and at elevated levels, demonstrating that the incorporation of a reactive natural pigment, such as anthocyanins, into a biopolymer matrix did not compromise its pH-dependent colour-changing ability.

3.2.3 | Sensitivity to Volatile Amines

As fish products begin to spoil, trimethylamine oxide (TMA-O), an osmolyte naturally present in fish, is enzymatically decomposed into DMA and TMA. Elevated concentrations of DMA, TMA and ultimately NH_3 are associated with the undesirable 'fishy' taste commonly encountered in stale fish products [49]. Therefore, the presence of these volatile compounds serves as an indication of fish spoilage, prompting the assessment of the smart labels to evaluate their response time. The smart labels were exposed to varying concentrations (0.002–1 M) of TMA, DMA and NH_3 solutions. The films exhibited colour changes under all tested conditions, as shown in Table 2.

The freshness stage of the fish ('fresh', 'moderate' and 'spoilt') was determined using the known mean spoilage threshold of NH_3 (35 mg/100 g fish) produced during spoilage of fish and comparing it with the concentrations of NH_3 used in this sensitivity analysis [50]. To calculate the molarity of NH_3 corresponding to a spoilage threshold of 35 mg per 100 g of fish, a theoretical approach was employed. The NH_3 mass was first converted to moles using its molecular weight (17.03 g/mol), yielding approximately 2.056×10^{-3} mol. Considering that fish tissue is approximately 70% water by weight, the molarity was calculated, resulting in a concentration of approximately 0.0293 M. This concentration was used as a reference for simulating fish spoilage in the label sensitivity evaluation. This NH_3 concentration corresponds to a colour change similar to the one provided between 0.02 and 0.2 M NH_3. According to Table 2, at the point of the expected fish spoilage, the colour of the smart label has turned from reddish-pink to colourless green.

To further understand the responsiveness of the smart labels to each volatile amine, a schematic comparison of the total colour difference (ΔE) is presented in Figure 5. Upon exposure to TMA and DMA, the smart labels demonstrated similar colour changes in terms of ΔE values; however, the colouration of the labels exposed to DMA appeared more intense (Table 2). The exposure of the labels to NH_3 solutions resulted in higher colour difference values (approaching 60) at all the tested concentrations, with the exception of the lowest (0.002 M). This phenomenon can be attributed to the intermolecular interactions affecting the volatility of each compound. NH_3 molecules are smaller and more polar, forming stronger hydrogen bonds due to the presence of an electronegative nitrogen atom and hydrogen atoms directly bonded to it. In contrast, TMA does not form hydrogen bonds, as its hydrogens are attached to carbon atoms, which are less polar.

In general, this test indicated that the fabricated smart labels were capable of sensing progressively increasing concentrations of volatile amines, which was reflected in an observable increase in colour change from reddish-pink to colourless-pale pink and finally to light green and yellowish-brown. The colour change of the smart labels was clearly visible within the first minute of the experiment and continued to intensify over time. Ameri et al. [51] in their study regarding the development of a colourimetric indicator based on black rice anthocyanin and polyethylene terephthalate performed a similar sensitivity test to TMA, DMA and ammonium hydroxide. They reported a transition in the film's colour, progressing from a red hue to a deep purple/blue shade and to a light brown/dark yellow tone.

3.2.4 | Microstructure Characterization

The films microstructure was examined using SEM at a magnification of 5000× (Figure 6A,C), employing an ETD in

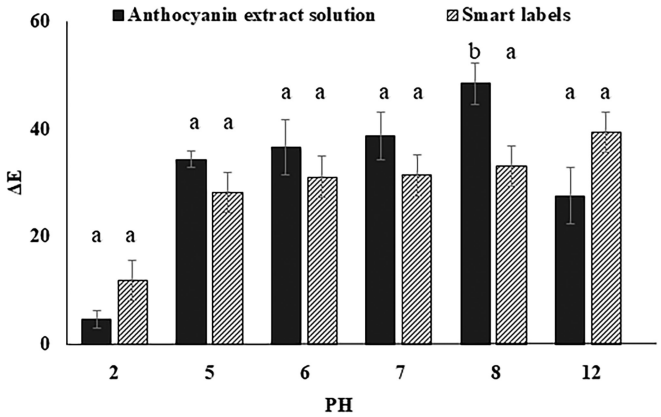

FIGURE 4 | Schematic comparison of the total colour difference (ΔE) observed after the exposure of the anthocyanin extract and the smart labels containing anthocyanin extract to pH 2–12 buffer solutions. Values with different superscripts (a, b) were significantly different as shown by Duncan's multiple range test ($p \leq 0.05$).

TABLE 2 | Digital images of the smart labels exposed to varying concentrations of TMA, DMA and NH_3 displaying the colour response and the anticipated freshness stage of the fish determined based on the NH_3 concentration.

	Control	0.002	0.02	0.2	0.4	0.6	0.8	1
TMA								
DMA		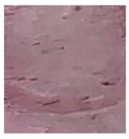						
NH_3								
Freshness stage	fresh	fresh	moderate	spoilt	spoilt	spoilt	spoilt	spoilt

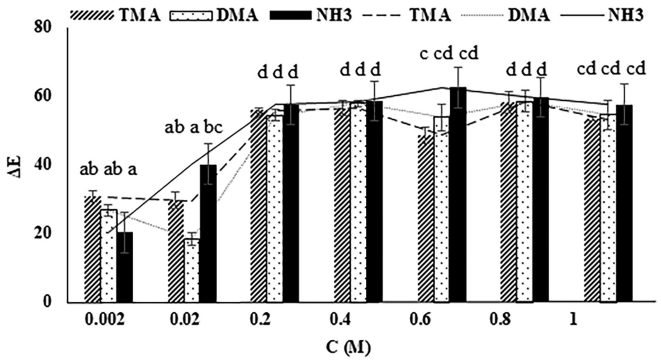

FIGURE 5 | Schematic comparison of the total colour difference (ΔE) observed after the exposure of the smart labels to different concentrations of TMA, DMA and NH_3. Values with different superscripts (a, b, c, d) were significantly different, as shown by Duncan's multiple range test ($p \leq 0.05$).

combination with HiVac mode to enable the detection of secondary electrons and to produce images of ultra high-resolution. PVA and starch appear to have bonded adequately, as proven from the homogenous surface of the control film. The blurred interface between the two polymers suggests the presence of strong bonding interactions. Tian et al. [52] and Patil et al. [15] have conducted comprehensive studies on the interactions between starch and PVA blends, reporting similar findings regarding the surface and cross-sections of the composite films. Concerning the PVA/starch/anthocyanin films, the SEM micrographs revealed adequate dispersion of the natural extract within the polymer matrix. A few small but evenly distributed micropores observed on the film surface indicate slight surface separation; however, the overall miscibility remained good. The compatibility of the materials was further confirmed through cross-section images at 1000× magnification (Figure 6B,D). The cross-sections confirmed the uniformity of the structure of PVA/starch/anthocyanin films and highlighted a slight separation phase within the PVA/starch films, which displayed some pores and folds. The folds revealed at the cross-sections of the PVA/starch films, which were not present in the PVA/starch/anthocyanin films, may suggest that anthocyanins acted as a cross-linking agent and reduced the phase separation. Qin et al. [29] studied the incorporation of anthocyanins on PVA/starch blends and stated that by incorporating compounds with pH sensitive charges such as anthocyanins could improve the miscibility of dissimilar polymers, as the counterions contribute to mixing entropy, promoting better compatibility.

3.2.5 | FT-IR

FT-IR spectroscopy (4000–600 cm^{-1}) was used to explore the physicochemical structure and intermolecular interactions

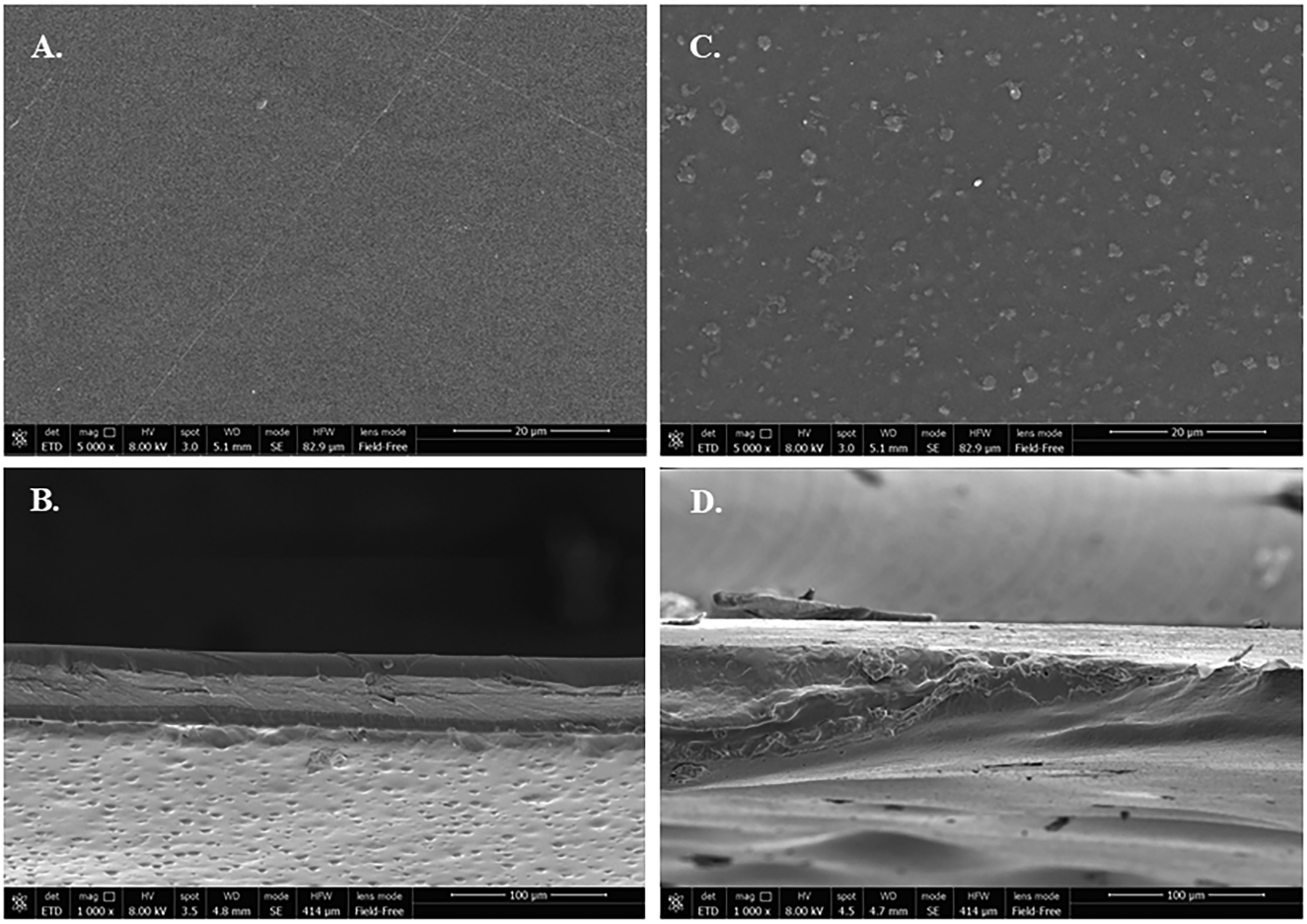

FIGURE 6 | SEM photographs of the surface (A) and cross-sections (B) of the PVA/starch (control) films and surface (C) and cross-sections (D) of the PVA/starch/anthocyanin films.

between the polymers and the anthocyanins (Figure 7). The absorption band around 3200–3500 cm^{-1} shows the O–H stretching. Both PVA/starch and PVA/starch/anthocyanin film spectra revealed broad O–H stretching bonding in the region of 3275–3277 cm^{-1}, which is a strong indicator of hydrogen bonding. The PVA/starch/anthocyanin film showed a 3275 cm^{-1} peak, which was shifted compared to the pure PVA/starch peak at 3277 cm^{-1}. This shift indicates that the incorporated anthocyanins are likely bonded to PVA and starch through hydrogen bonding, thus resulting in a denser polymeric structure.

The peak value at 2930 cm^{-1} that is associated with both PVA and starch reinforces the aliphatic C–H stretching. It serves as an indicator of the presence of the polymer backbone. The PVA/starch/anthocyanin film features a 2930 cm^{-1} peak value that is slightly higher than pure PVA/starch (2921 cm^{-1}). This small modification of the peak could be attributed to the introduction of anthocyanins within the polymer structure.

The band at 1651 cm^{-1} (C=O and C=C stretching) found in PVA/starch/anthocyanins but not in the pure PVA/starch film likely corresponds to C=O stretching (carbonyl groups), along with C=C vibrations from anthocyanins, and shows that anthocyanins are successfully incorporated in the polymer matrix. This confirms that all anthocyanins contain a conjugated carbonyl ring and an aromatic ring. Wang et al. [53] reported similar peaks in their smart films containing anthocyanins, such as C=C aromatic ring stretching vibrations around 1640 cm^{-1}. The peak at 1734 cm^{-1} in the PVA/starch film probably comes from the leftover acetate groups in PVA. As there was no peak at 1734 cm^{-1} in the PVA/starch/anthocyanin film, anthocyanin interactions might have changed or lessened the remaining acetate groups in PVA.

The peak at 1419 and 1335 cm^{-1} correspond to CH_2 bending vibration in PVA and starch molecules, respectively. The 1335 cm^{-1} band could be related to any C–O–H deformation of starch. In PVA/starch/anthocyanin film, peaks appeared at 1419 cm^{-1} in addition to 1335 cm^{-1}, whereas in pure PVA/starch film, peaks occurred at 1372 cm^{-1} along with 1247 cm^{-1}. These shifts clearly indicate structural modifications as anthocyanins were fully incorporated in the polymer matrix, affecting the way starch interacted with PVA molecules. According to Pereira et al. [54], changes that appear in the region of 1500–1600 cm^{-1} with a clear increase in the intensity of the bands in this region indicate the successful incorporation of anthocyanins into the polymer matrix.

Both film categories showed a peak around 998–994 cm^{-1}, and this relates to C–O–C stretching. The starch glycosidic linkages' C–O vibrations and C-C stretching of C–O–C groups usually

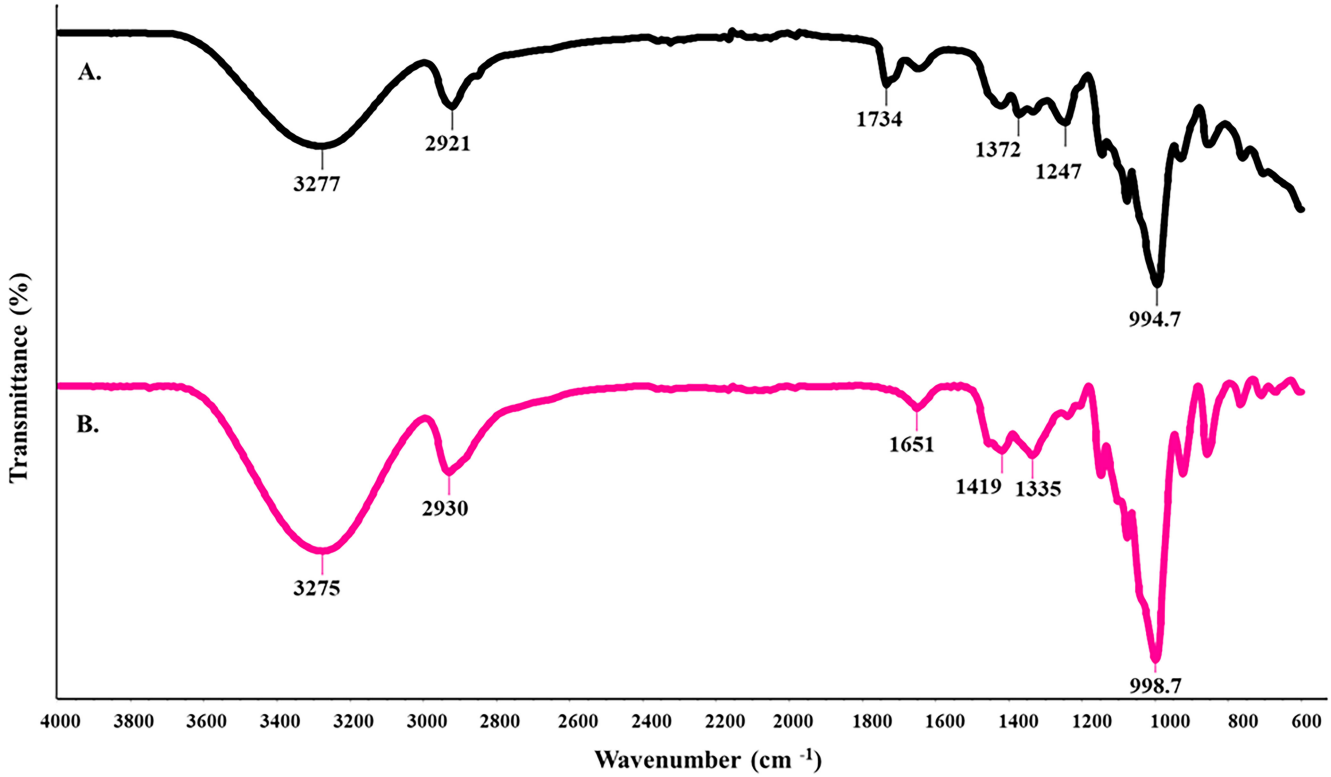

FIGURE 7 | FT-IR spectra of PVA/starch (control) (A) and PVA/starch/anthocyanin (B) films.

TABLE 3 | MC (%), TSM (%) and SI (%) obtained for control and smart labels.

Sample	MC %	TSM %	SI %
PVA/starch (control)	11.52 ± 0.9^{b}	74.18 ± 3.88^{a}	183.24 ± 7.88^{b}
PVA/starch/anthocyanin	9.21 ± 0.6^{a}	70.67 ± 4.88^{a}	47.69 ± 1.63^{a}

Note: Values are expressed as mean ± standard deviation. Values with different superscripts in the same column (a, b) were significantly different as shown by Duncan's multiple range test ($p \leq 0.05$).

result in the appearance of this peak around 1000 cm^{-1} [52], indicating the existence of polysaccharides in the film matrix. The shift from 994.7 to 998.7 cm^{-1} in the PVA/starch/anthocyanin film suggests that anthocyanins possibly interacted with starch through the hydroxyl groups.

Overall, both spectra revealed a homogeneous polymer network, which is crucial for film integrity and functional properties. Hydrogen bonding was stronger in the PVA/starch/anthocyanin films, as evidenced by the slight shift in the O–H stretching peak (~3275 cm^{-1}), indicating that anthocyanins formed stronger intermolecular interactions with the film matrix, a finding that is also supported by SEM analysis. This could be explained by the fact that anthocyanins' hydroxyl groups formed hydrogen bonding interactions with the hydrophilic groups of starch, PVA and glycerol [29]. Several researchers have reported similar structural changes following the incorporation of anthocyanin into films [37, 55].

3.2.6 | MC, WS and SI

The fabricated films were evaluated for physical properties, including MC, WS and SI, to determine the water interactions of the molecules and their potential impact on the functional properties of the labels. The results obtained are presented in Table 3.

The control films consisting of PVA and starch presented a high SI, possibly attributed to the high degree of swelling exhibited by PVA in water [56]. PVA molecules swell considerably because of their hydrophilic hydroxyl groups, non-crystalline structure and ability to form hydrogen bonds with water [57]. These interactions lead to the absorption and retention of water by multiple polymer chains, leading to significant expansion. The incorporation of the anthocyanin extract into the PVA/starch matrix resulted in a decrease in the SI of the films; however, it did not appear to affect WS, as the difference was not statistically significant. This finding is consistent with observations reported by numerous researchers regarding the incorporation of anthocyanin extracts into water-soluble membranes [58, 59]. For example, Jayakumar et al. [60] studied the swelling capacity of PVA/chitosan smart films and found that it decreased sharply from 209.5 ± 0.4 to 67.9 ± 0.5 after the incorporation of sweet purple potato anthocyanins into the polymer matrix. The incorporation of anthocyanins into the films considerably increased the number of cross-linking points between the polymer chains, because anthocyanins possess numerous hydroxyl groups that can form hydrogen bonds with the polymer chains [61]. This observation was also evident in the FT-IR analysis of the films. The restriction of chain movement reduced the polymer's ability to expand and absorb significant amounts of water, leading

to a lower swelling degree. A lower SI indicates lower water absorptivity and thus higher stability of the smart labels. As for the WS of the films, it was found comparably higher than similar smart films based on red grape skins anthocyanins, probably attributed to the polymers selected. Specifically, Ran et al. [36] in their study about pH-colourimetric films based on soy protein isolate/ZnO nanoparticles and grape-skin red reported WS values ranging between 22.2% and 27.2% with the addition of anthocyanins significantly decreasing the WS. A slight decrease in WS after anthocyanins incorporation was also observed in this work, but it was not found statistically significant, possibly due to the fact that anthocyanins have a less pronounced effect on WS compared to the primary film-forming components, PVA and starch.

3.2.7 | Wettability

The water contact angle (WCA) is generally considered a precise index of the wettability of a film [62]. WCA values lower than 90° characterize materials as hydrophilic, whereas values higher than 90° indicate hydrophobic materials. Figure 8 presents the wettability of the control (A) and smart labels (B), which exhibited WCA values of $\theta_c = 82.78° \pm 8.10°$ and $\theta_s = 82.39° \pm 7.44°$, respectively.

Both film categories (with and without anthocyanin extract) demonstrated a moderately hydrophilic profile ($\theta < 90°$), which is in agreement with the WS results. Although both PVA and starch are hydrophilic polymers, the WCA values were relatively close to 90°. Similar findings were reported by Patil et al. [15], who noted WCA values of PVA/starch membranes that were slightly below 90°. That observation may be attributed to surface factors such as the surface roughness [63]. In the case of smart labels, the WCA could also be explained by the incorporation of anthocyanins, which may have partially functioned as a cross-linking agent and blocked several hydrophilic groups of the polymer matrix, reducing the bonding with water molecules [20]. On the other hand, partial hydrophilicity is a desired feature because it facilitates the rapid diffusion of hydrogen ions and hydroxide ions into the fibrous structure and interacts with anthocyanins, resulting in colour responses to different pH values [64]. Overall, these results are encouraging, as they suggest low porosity of the films (indicating that droplets do not penetrate easily) and relatively reduced wettability.

3.3 | Storage of Smart Films

3.3.1 | Adsorption Isotherms of Films During Storage

The moisture sorption isotherms of all the films stored under different conditions exhibit sigmoidal curves, characterized by a gradual initial increase in moisture at low water activity values ($a_w < 0.7$) and an exponential increase at higher water activity values ($a_w > 0.75$). Storage temperature appeared to influence the moisture sorption of smart labels, with the films stored in lower temperatures demonstrating greater adsorptive capacity, especially in higher a_w environments ($a_w > 0.75$). At a storage temperature of 25°C, the incorporation of the anthocyanin extract affected the sorption behaviour of the films by increasing the moisture sorption (g water/g dry base) in all tested a_w environments. Similar results were observed at 15°C, except for the $a_w = 0.9$ storage environment, where control films appeared to be more adsorptive. For the samples stored at 5°C, smart labels were more adsorptive than the control ones after the $a_w = 0.34$ environment. The adsorption isotherms are displayed at Figure 9.

GAB model was used to describe experimental data to better understand the moisture sorption of the films. GAB equation has a similar form to Brunauer–Emmett–Teller (BET) equation, with an extra constant, k, which improves adaptation to a wider range of moisture contents than BET ($a_w > 0.9$). Therefore, given the values of the k parameter were close to 1 ($0.92 < k < 1$), both models could adequately describe the current experimental data. All the GAB parameters are presented in Table 4. The R^2 coefficients (≥ 0.95) reveal that the GAB model described satisfactorily the adsorption of water in all tested films.

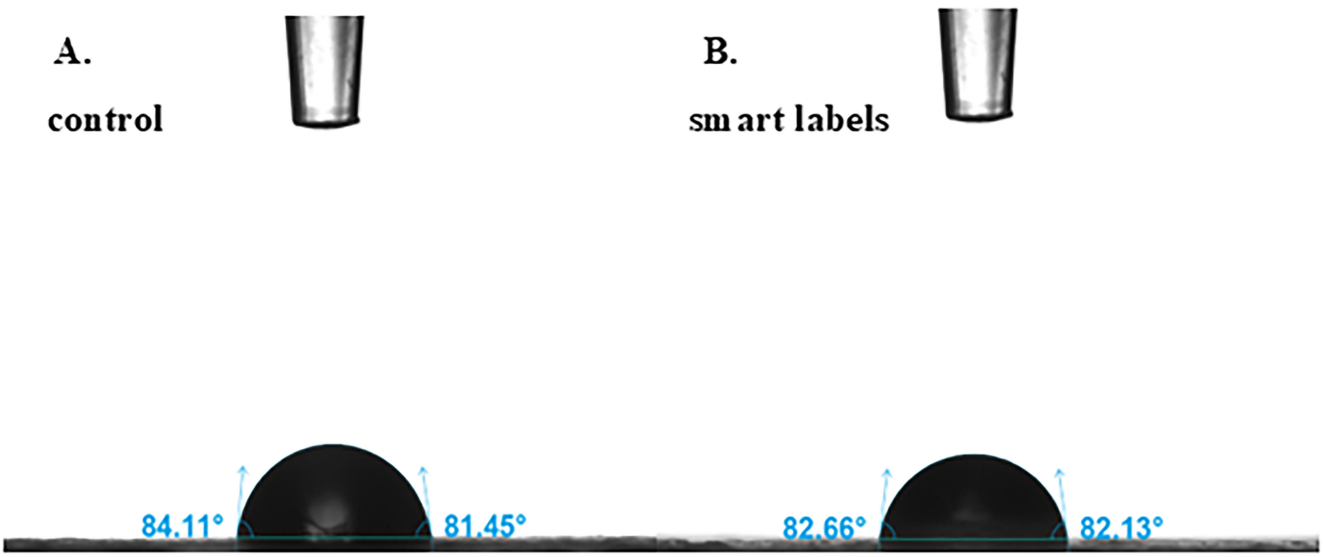

FIGURE 8 | WCA of the control (A) and smart labels (B) provided by the Theta Flow Optical Tensiometer camera.

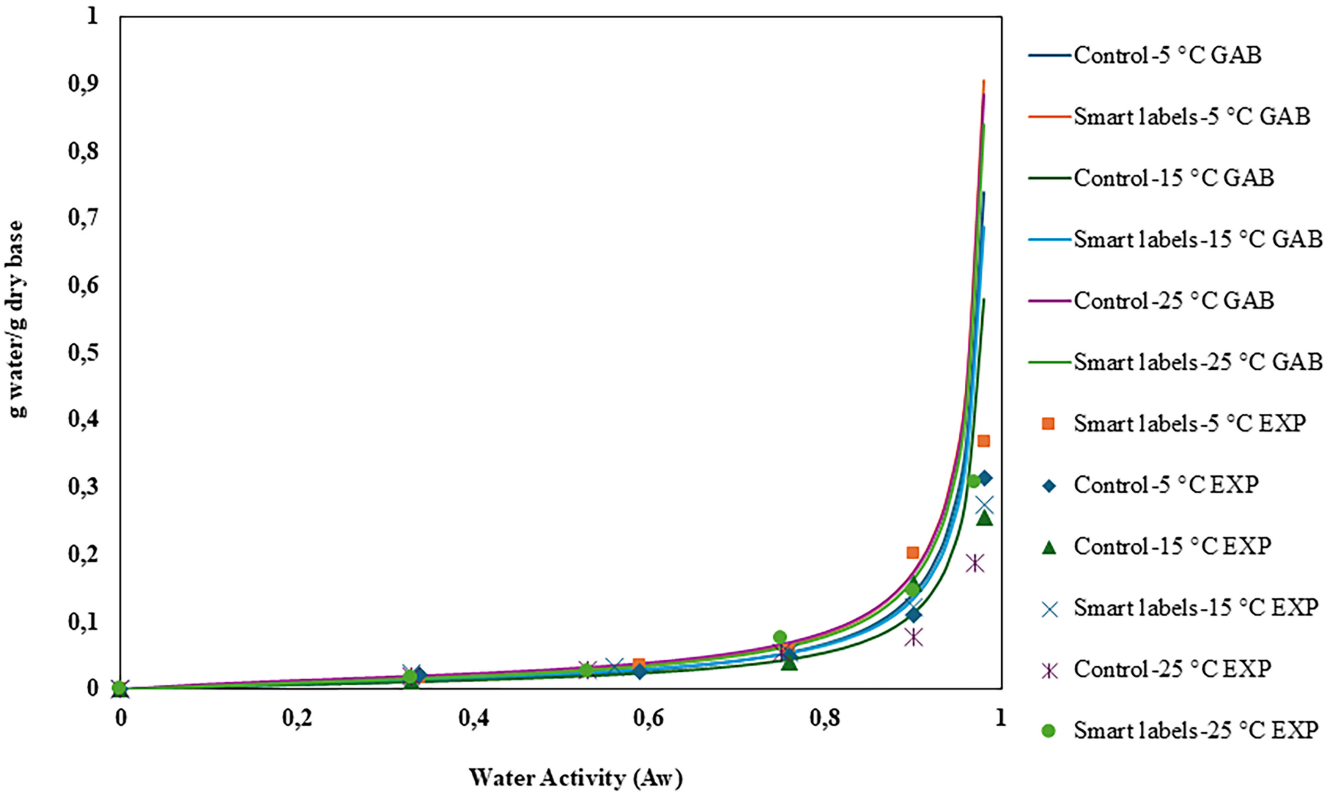

FIGURE 9 | Moisture sorption isotherms of the control and smart labels at all storage conditions (5°C, 15°C and 25°C).

TABLE 4 | GAB model parameters for control and smart labels at all storage temperatures (M_0 represents the monolayer value in g water/g solids, and C and k are the GAB constants).

Storage temperature	Sample type	M_0	k	C	R^2
5°C	Control	0.0146 ± 0.0015^{bc}	0.97 ± 0.03^{a}	2.75 ± 0.28^{a}	0.99
	Smart labels	0.0181 ± 0.0011^{d}	0.98 ± 0.04^{a}	2.72 ± 0.09^{a}	0.98
15°C	Control	0.0116 ± 0.0012^{a}	0.99 ± 0.01^{a}	4.64 ± 1.39^{bc}	0.97
	Smart labels	0.0135 ± 0.0012^{ab}	0.98 ± 0.01^{a}	6.82 ± 1.55^{cd}	0.99
25°C	Control	0.0165 ± 0.0021^{cd}	0.92 ± 0.05^{a}	7.22 ± 1.16^{d}	0.95
	Smart labels	0.0167 ± 0.0013^{cd}	0.99 ± 0.01^{a}	3.92 ± 0.35^{b}	0.95

Note: Values are expressed as mean ± standard deviation. Values with different superscripts in the same column (a, b, c, d) were significantly different as shown by Duncan's multiple range test ($p \leq 0.05$).

The monolayer value (M_0) represents the approximate amount of water required to form a layer of one molecular thickness on the highly polar groups of the dry film (approximately 1 mol of water per mole of highly polar groups). This water is immobile, cannot serve as a solvent and behaves as part of the solid [37]. Small M_0 values indicate a limited number of active sites available for water binding [65]. The highest M_0 value was obtained in the smart labels stored at 5°C, which may be attributed to the enhanced interactions between water molecules and the film structure at lower temperatures, leading to higher monolayer values. Several researchers have reported that the GAB monolayer value tends to decrease with increasing temperature [66].

The C constant in the GAB model is related to the difference in free enthalpy between the molecule in the first layer and those in subsequent layers. This parameter offers a quantitative assessment of the binding energy differences between multilayer adsorption and condensation. The incorporation of anthocyanins into the PVA/starch matrix did not appear to significantly affect the C constant, except for the films stored at 5°C, where the smart labels displayed a statistically significant lower C value, indicating a weaker binding force of water to the materials. This phenomenon may be attributed to the fact that anthocyanins occupied or blocked some of the primary water-binding sites on the starch or PVA molecules, a finding that has been also reported by other researchers for chitosan/anthocyanin smart films, where anthocyanins were also extracted from grapes [67].

In general, the sorption isotherm experiments highlighted the importance of storage conditions for films based on biodegradable materials, such as starch and PVA, which are inherently hydrophilic. Both RH and temperature influenced significantly

the stability of the films and consequently, their shelf life. After 45 days of storage, it was evident that the shelf life of the films was reduced when stored under lower temperature and higher RH conditions due to the increased moisture sorption capacity, which accelerated the rate of deterioration of the films.

3.3.2 | Colour and Light Barrier Properties of Films During Storage

Control films and smart labels were stored at three different temperatures (5°C, 15°C and 25°C) and five RH (33%, 56%, 75%, 90% and 98%) environments for 15, 30 and 45 days. At predetermined time intervals, films (with 5 replicates) were removed from each storage environment and evaluated for their visual properties. The light absorbance results for the PVA/starch and PVA/starch/anthocyanin films under all storage conditions are presented in Figures 10 and 11, respectively.

It is evident from Figure 10 that during the 45-day storage of PVA/starch films, a slight increase in light absorbance was observed, which correlated with the duration of storage. The optical parameters of the films were expected to change as a result of the light scattering caused by water uptake. Because the films under higher humidity conditions absorbed more water, the light absorbance also increased. At 5°C, this finding was particularly pronounced at the end of the storage period (45 days) for films stored at RH 90% and 98%, a finding that is consistent with the adsorption isotherms. Practically, this implies that the control films became opaquer and absorbed more light as a result of increased water uptake.

It is known that anthocyanins have two characteristic absorption peaks at a wavelength region of 260–280 nm (UV light) and 490–550 nm (visible light). The intensity of the absorption of the films under each storage condition (a_w-temperature) can provide important insight into the colour retention and integrity of the smart labels. Generally, the highest light absorbance was observed at lower a_w conditions, regardless of the storage temperature. When stored at the highest a_w environment (98%), the smart labels that retained their colour intensity most adequately were those stored at 25°C, whereas at RH 90% the film colour was retained similarly at both 15°C and 25°C. At the end of the storage period (45 days) at 5°C, the highest light absorbance around the wavelengths corresponding to anthocyanin absorption was noted at the films stored at RH 56% > 33% > 75% > 90% > 98%. This indicates that the smart labels stored at 5°C begin to lose their colour intensity when kept in higher RH environments. Ran et al. [36] in their study about colourimetric films based on soy protein isolate/ZnO nanoparticles and grape-skin red observed that films stored at 4°C exhibited superior colour stability than films stored at 25°C, a finding that was consistent with the results of Sinela et al. [68]. However, these studies did not include intermediate temperatures. The current study suggested that better colour preservation of the smart labels was observed at the intermediate storage temperature of 15°C, especially for films stored in environments with increased RH. Relevant research by Zhai et al. [19] investigated the colour stability of smart PVA/starch/anthocyanin films stored for 14 days at 4°C and 25°C under 75% RH, concluding that colour was more efficiently maintained at 4°C, albeit with only a small difference from 25°C.

3.3.3 | WS of Films During Storage

During the storage experiment, TSM % of all films was measured at 15, 30 and 45 days to determine how the different

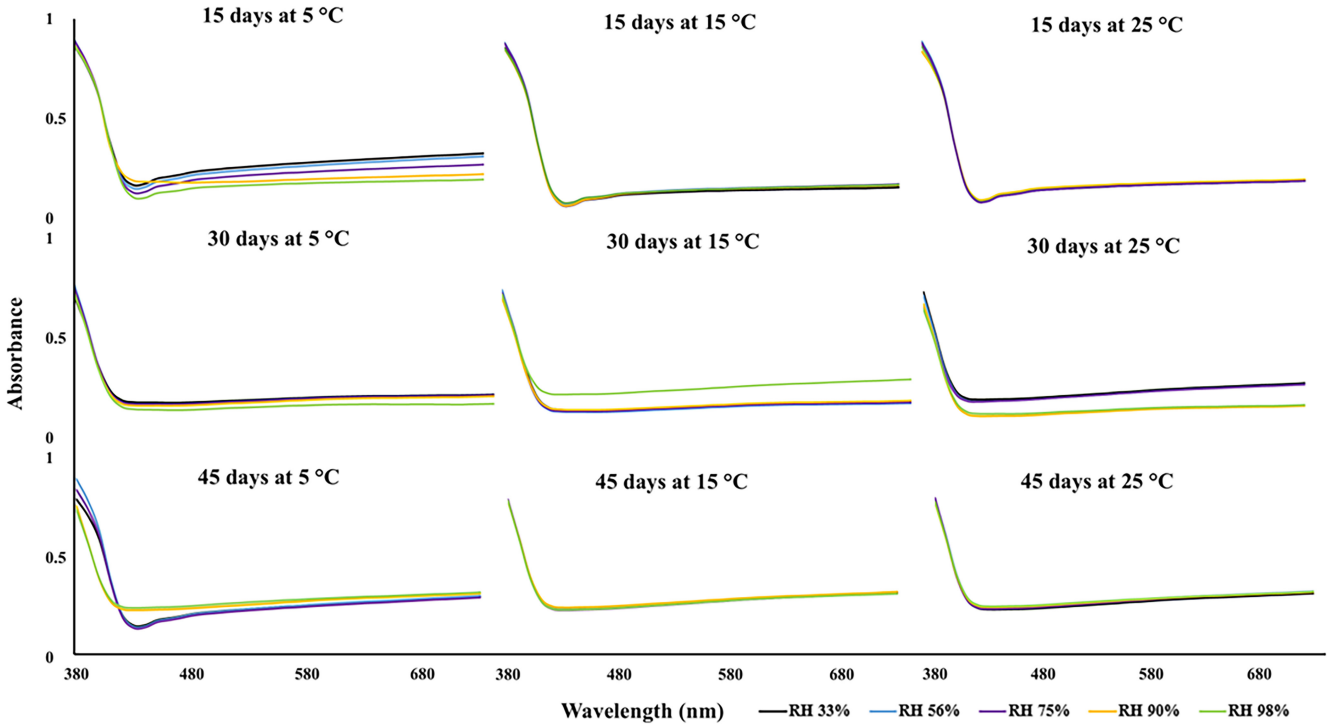

FIGURE 10 | Light absorbance of PVA/starch films stored at different temperatures (5°C, 15°C and 25°C) and RH conditions (33%, 56%, 75%, 90% and 98%) after 15, 30 and 45 days of storage.

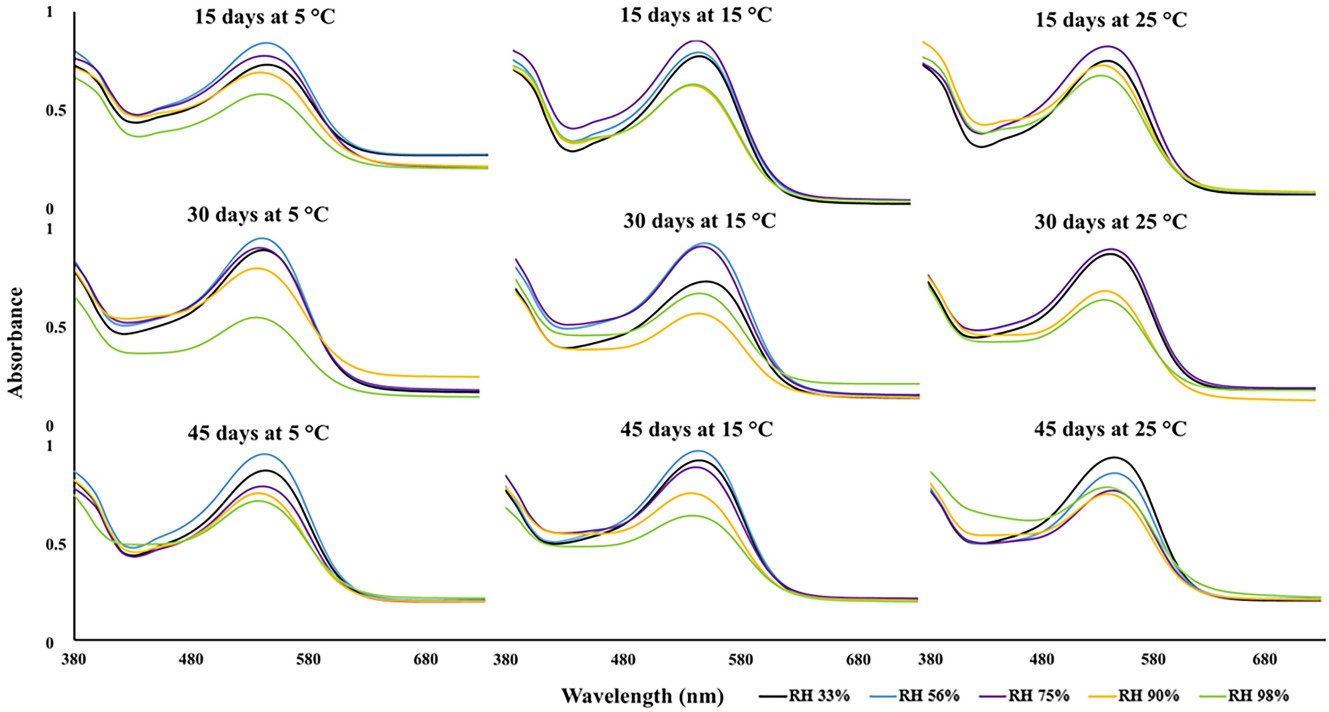

FIGURE 11 | Light absorbance of PVA/starch/anthocyanin films stored at different temperatures (5°C, 15°C and 25°C) and RH conditions (33%, 56%, 75%, 90% and 98%) after 15, 30 and 45 days of storage.

storage conditions affected the films WS. Figure 12 presents the TSM % for control and smart labels stored at 5°C, 15°C and 25°C under RH conditions of 33%, 56%, 75%, 90% and 98%.

During the first 15 days of storage at 5°C, all films exhibited a decrease in TSM % as the RH of storage increased (i.e., TSM of smart labels was 75% at RH 33% and decreased to 36% at RH 98%). For control films stored at 15°C and 25°C, the TSM % values did not vary significantly between the two temperatures, except for the ones stored at RH 56%, where WS was considerably higher at 25°C. For smart labels stored at 15°C and 25°C, the TSM % values showed statistically significant differences only in the 90% and 98% RH environments, with TSM % values nearly doubling at 25°C.

After 30 days of storage, the solubility of the control films did not differ significantly between the three storage temperatures but was enhanced compared to the first 15 days of storage. Regarding the smart labels, the TSM % values at 5°C and 25°C did not differ significantly and were relatively higher than those recorded during the initial 15 days of storage. The smart labels stored at 15°C presented the lowest WS values (approximately 50% TSM), apart from the ones stored at 98% RH environment (80% TSM).

After 45 days, both control and smart labels displayed reduced WS compared to 15 and 30 days of storage. The high peak of TSM % at 30 days of storage, observed at all storage conditions, may be attributed to the amount of water that films had absorbed at that time. According to several researchers [47, 69], higher WS is anticipated when films have not yet reached the maximum water uptake, as this allows the polymer chains to disperse in the surrounding water. The TSM % values suggest that at 30 days of storage, the films had not yet reached the maximum water uptake threshold. After 45 days, the films absorbed a greater amount of water, leading to lower WS. Once again, films kept at 15°C displayed the most uniform TSM % values, regardless of the RH environment.

3.3.4 | Wettability of Films During Storage

WCA measurements were conducted during film storage to investigate the effect of the storage conditions on the wettability of the films. Figure 13 illustrates the WCA values of both control and smart labels obtained during the storage experiment where the respective water droplets depicted on top of each WCA bar for visual comparison.

In general, films conditioned in lower RH environments ($a_w < 0.75$) appeared to be more hydrophobic ($\theta > 90°$). In the case of control films, storage RH appeared to be the dominant factor for film wettability, having a clear negative correlation with WCA values at all tested temperatures (downward trend of WCA values when increasing a_w). At 90% and 98% RH environments, control films at all tested temperatures were significantly more hydrophilic (θ around 45°–60°) than the respectively conditioned smart labels (θ around 65°–80°). Smart labels did not present significant variances in the distribution of WCA values between the tested a_w storage conditions at 5°C and 15°C. However, smart labels stored at 25°C were found to be more hydrophilic at higher (90% and 98%) RH environments. At the end of the storage period (45 days), the smart labels were slightly less hydrophobic than at 15 and 30 days of storage. However, overall, the storage duration did not appear to have a clear and significant effect on the wettability of the films, as no statistically significant differences were observed for the smart labels stored for 15 and 30 days or for any of the control films.

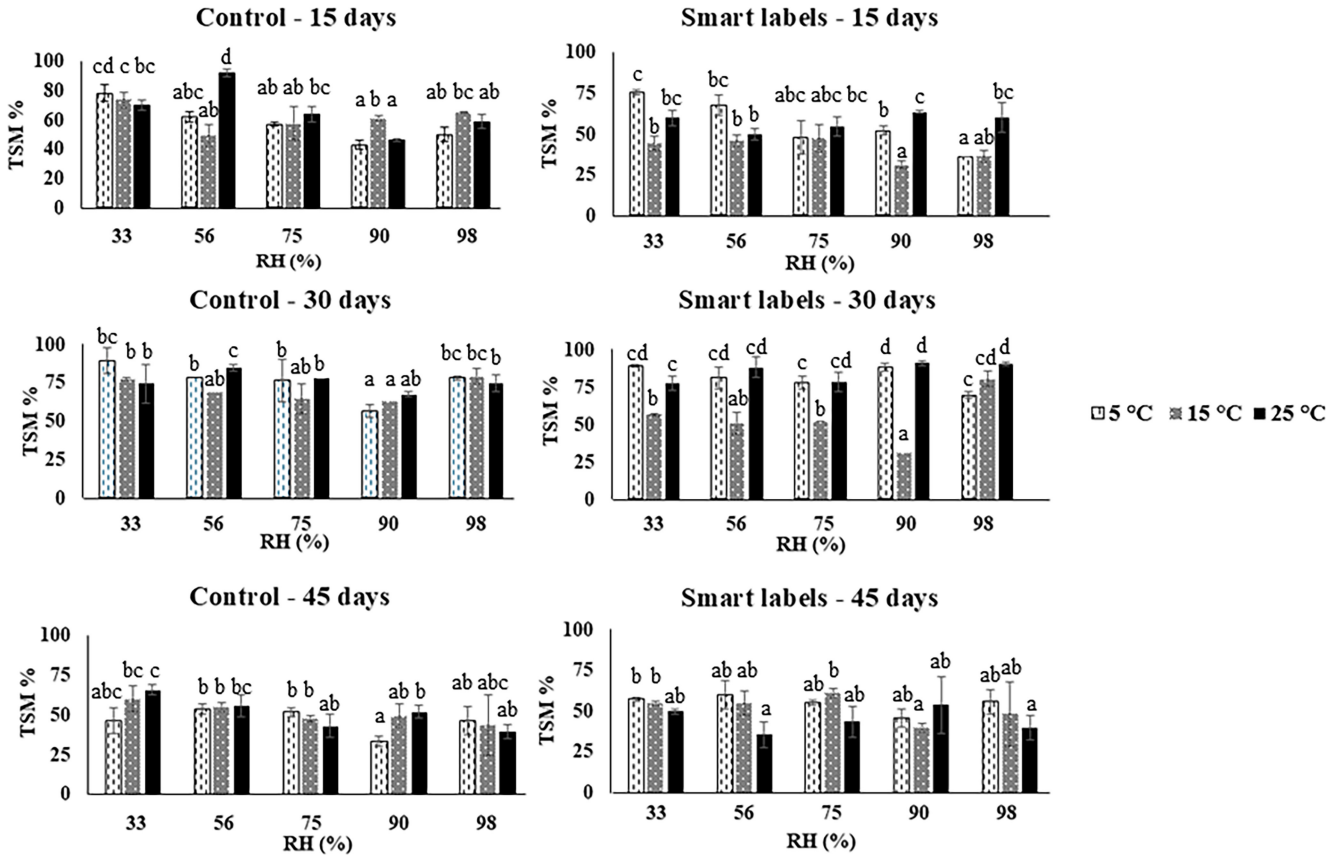

FIGURE 12 | TSM % of PVA/starch (control) and PVA/starch/anthocyanin (smart) films stored at different temperatures (5°C, 15°C and 25°C) and RH conditions (33%, 56%, 75%, 90% and 98%) after 15, 30 and 45 days of storage. Values with different superscripts (a, b, c, d) in each figure were significantly different as shown by Duncan's multiple range test ($p \leq 0.05$).

3.4 | Fish Freshness Monitoring

3.4.1 | Storage of Fish Under Constant and Variable Temperature Conditions

Fresh gilthead sea bream (*S. aurata*) fillets were stored for 9 days at constant (isothermal) and variable temperature conditions. Figure 14 presents the time–temperature profiles for both storage conditions during the fish shelf life experiments.

The quality parameters associated with the constant storage temperature (1.7°C) and variable temperature conditions (0°C–25°C) of fish stored in sealed pouches with smart labels attached inside the headspace of the pouches are presented and discussed below.

3.4.2 | Microbial Growth

The initial microbial load of the fish samples expressed by total viable counts (TVC) was 3.78 log cfu/g (day 0) and reached 7.62 ± 0.3 log cfu/g at storage day 9 at constant temperature conditions, whereas for variable storage conditions, TVC reached 7.37 ± 0.3 log cfu/g at storage day 7. *Pseudomonas* spp. exhibited a significantly higher growth rate in fish fillets stored under variable temperature conditions ($1.103 \pm 0.052\,d^{-1}$) compared to constant temperature conditions ($0.348 \pm 0.011\,d^{-1}$), as determined by the Baranyi model, which was used to fit the microbial growth curves and assess growth kinetics. However, following oxygen depletion inside the package (after Day 5), *Pseudomonas* spp. populations were eliminated, allowing for the rapid proliferation of other anaerobic microorganisms, such as Enterobacteriaceae [70]. The effective temperature, T_{eff}, determined by Arrhenius kinetics for the variable storage conditions of fish was 6.15°C. Growth kinetics for all microorganisms ($R^2 > 0.90$) are presented in Table 5.

Considering the acceptable limits for microbial contamination of 7 log cfu/g for TVC [71], the shelf life of sea bream fillets stored isothermally at 1.7°C was calculated as 7–8 days, whereas for fillets at variable conditions the shelf life was 5–6 days. Figure 15 presents the growth curves of spoilage microorganisms throughout the storage test of gilthead sea bream fillets. Based on the calculated log cfu/g of the microorganisms, the characterization 'fresh' (< 4 log cfu/g), 'moderate' (4–7 log cfu/g) and 'spoilt' (> 7 log cfu/g) was used for describing the freshness state of the fish fillets [72].

3.4.3 | pH and TVB-N Content

The pH of fish flesh varied between 6.5 and 6.7 for both storage conditions. A slight decrease in pH was observed during the

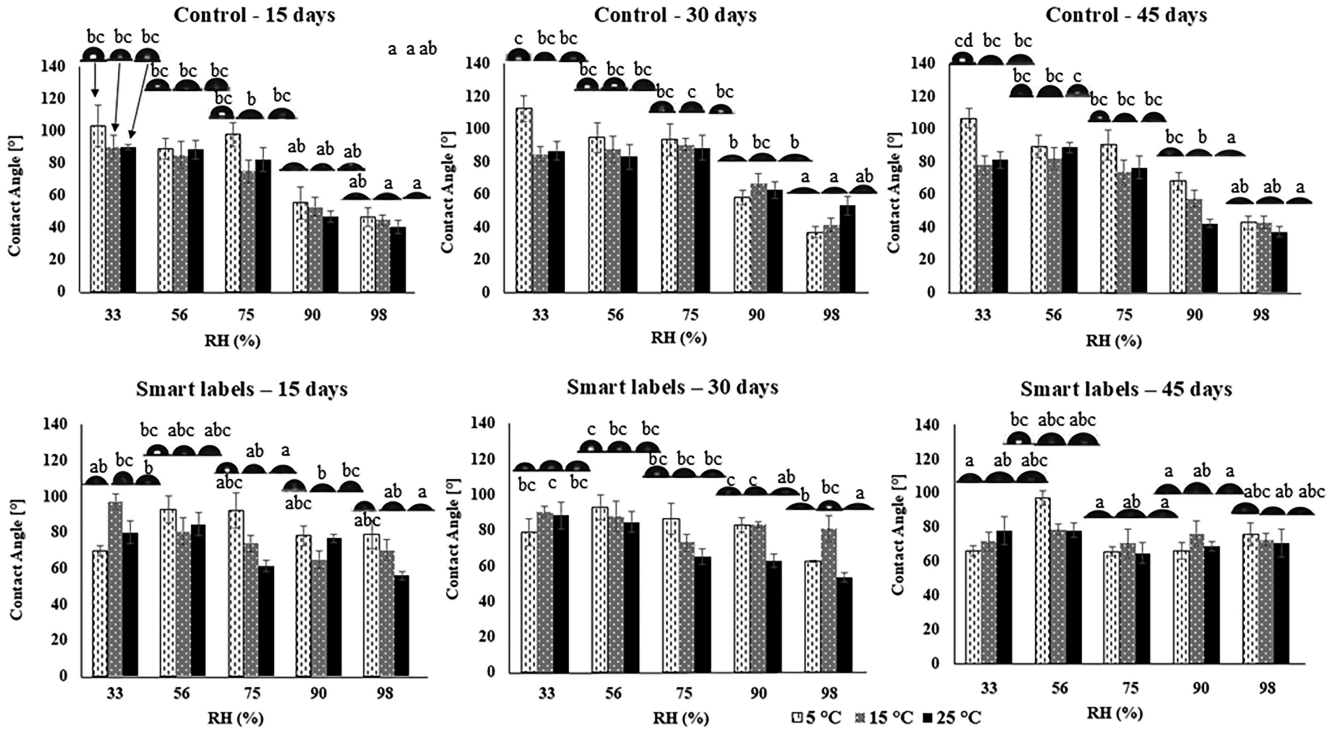

FIGURE 13 | WCA of control and smart labels stored at different temperatures (5°C, 15°C and 25°C) and RH conditions (33%, 56%, 75%, 90% and 98%) after 15, 30 and 45 days of storage provided by the Theta Flow Optical Tensiometer camera. On top of each WCA measurement bar, the respective droplet is presented. Values with different superscripts (a, b, c, d) in each figure were significantly different as shown by Duncan's multiple range test ($p \leq 0.05$).

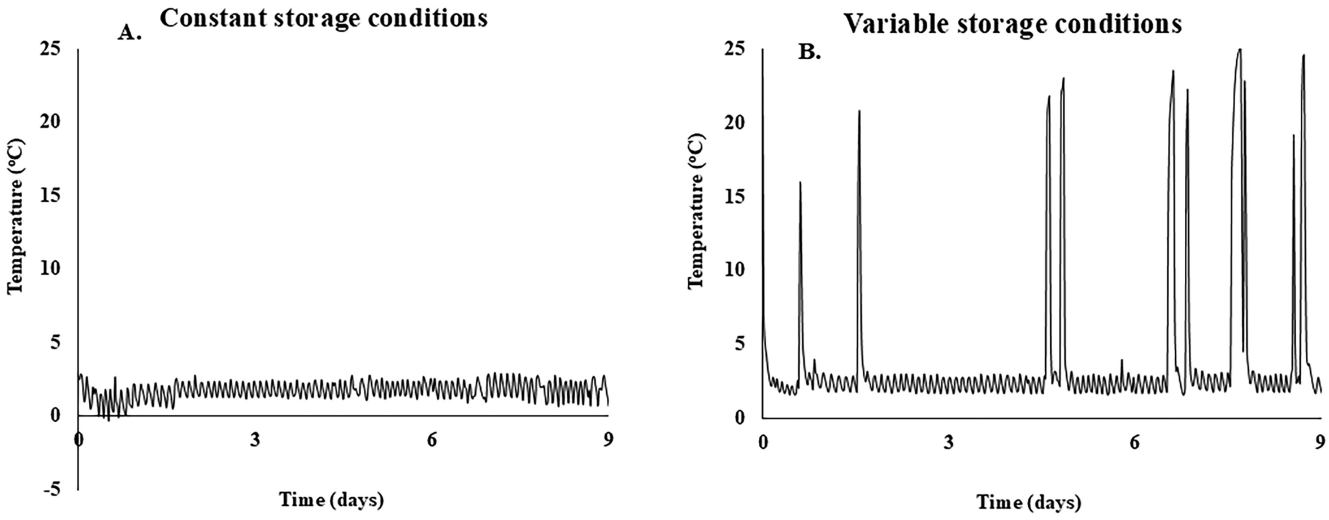

FIGURE 14 | Temperature fluctuations during the 9-day storage period of fish at constant (1.7°C) (A) and variable (B) temperature conditions for fish shelf life monitoring.

initial hours of storage (24-40 h), possibly attributed to autolytic reactions occurring within the fish flesh. The pH then increased progressively from 6.58 to 6.67 as the fish spoiled up to approximately 6–7 storage days. From Days 7 to 9, another pH decrease in pH was observed (6.56), primarily due to the accumulation of CO_2 in the package, which temporarily produced carbonic acid upon reacting with water molecules (as in-package moisture increased during fish storage), but also due to the proliferation of lactic acid bacteria accumulation [73].

TVB-N associated with volatile amines produced during fish spoilage such as TMA, DMA, and NH_3 was initially calculated at 7.29 mg/100 g and increased gradually during storage, reaching 23.50 and 25.80 mg/100 g by day 9 of storage at constant and

variable temperatures. TVB-N values of fish fillets were generally higher at all time intervals during storage at variable temperature, indicating faster spoilage rates.

3.4.4 | In-Package Gas Composition

The composition of the in-package headspace underwent continuous changes during fish spoilage (Figure 16). The O_2 concentrations decreased from 20.95% on storage day 0 to 1.45% at the end of storage (Day 9) under constant temperature conditions, followed by a characteristic increase in CO_2 concentrations, which rose from 0.93% on Day 0 to 6.8% on Day 9. At the end of the storage period under variable temperature conditions, the O_2 and CO_2 concentrations were 0% and 10.85%, respectively. The increase in CO_2 is attributed to microbial metabolic activity, which was more pronounced in fish stored under variable temperature conditions, resulting in a faster increase in headspace CO_2 (e.g., on Day 6 of storage, CO_2 concentrations were 4.9% and 12.1% at constant and variable storage conditions, respectively).

3.4.5 | Colour Response of Smart Labels

The smart labels exhibited a significant colour change during fish storage under both storage conditions, transitioning from

TABLE 5 | Baranyi parameters (i.e., k = growth rate (d^{-1}), N_{max} = maximum population at the end of storage (log cfu/g) and R^2 = coefficient of determination) of microbial growth in sea bream fillets stored under constant (1.7°C) and variable (0°C–25°C) conditions.

Storage temperature	Microorganism	k (d)	N_{max} (log cfu/g)	R^2
Constant (1.7°C)	TVC	0.445 ± 0.025	9.14 ± 0.70	0.996
	Pseudomonas spp.	0.348 ± 0.011	5.79 ± 0.41	0.901
	Enterobacteriaceae	0.714 ± 0.068	8.16 ± 0.82	0.929
Variable	TVC	0.634 ± 0.044	10.44 ± 0.59	0.926
	Pseudomonas spp.	1.103 ± 0.052	6.56 ± 0.55	0.904
	Enterobacteriaceae	0.520 ± 0.050	8.47 ± 0.49	0.934

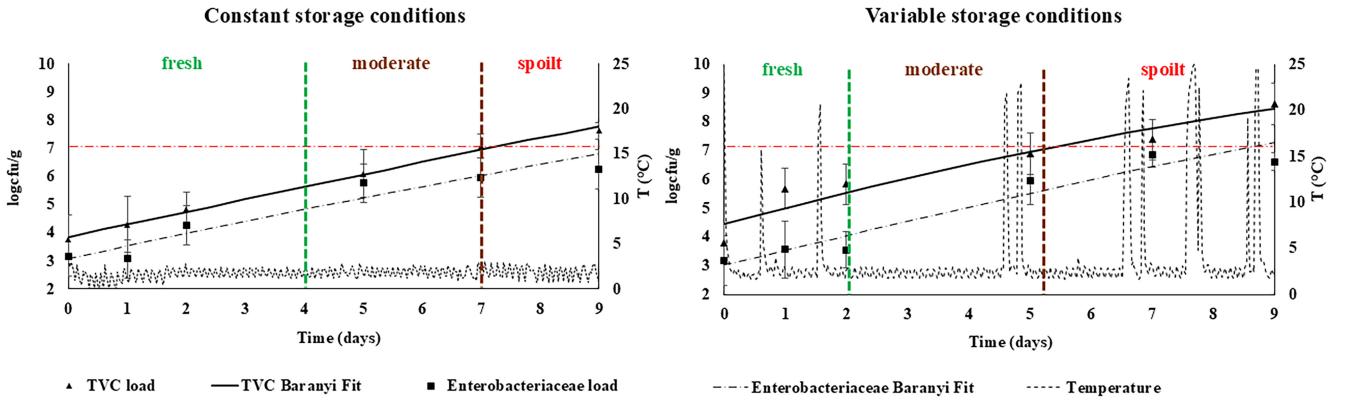

FIGURE 15 | Microbial growth of TVC and Enterobacteriaceae during storage of gilthead sea bream fillets at constant (1.7°C) and variable temperature conditions.

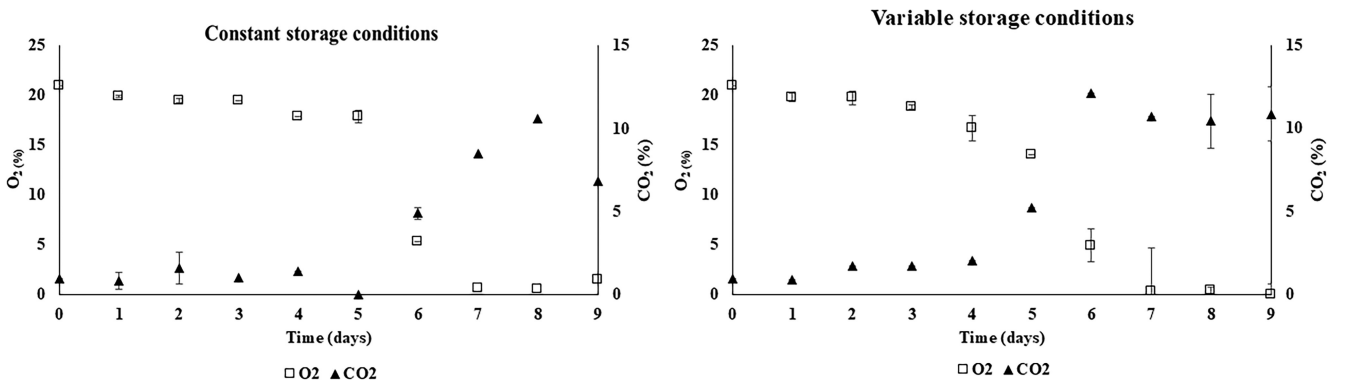

FIGURE 16 | Headspace composition during storage at constant (1.7°C) and variable temperature conditions of gilthead sea bream fillets.

pinkish-red on day 0 to light purple (colourless), then to light green, and finally to pale bluish-grey by Day 9. As indicated by the colour measurements of the smart labels, the a-value (reflecting the red hue) consistently decreased during the storage experiment, with a more pronounced decline observed under variable storage conditions. Specifically, the a-value decreased from 52.95 on Day 0 to 32.11 and 19.94 under constant and variable temperature conditions, respectively, with the latter corresponding to a faster spoilage of the fish. The colour parameter b (reflecting the yellow hue) in the smart labels decreased during fish storage, with values dropping from −1.29 at Day 0 to −7.85 and −6.10 at constant and variable temperature conditions, respectively. This indicates that the colour of the films shifted more towards the green-blue spectrum. The lightness of the films remained unchanged (with no statistically significant difference) during the initial days of storage, after which it increased slightly. Similar colour changes were observed when smart films from polyvinyl alcohol/palmyra root sprout, carbon dots and anthocyanins were developed by Koshy et al. [74] to monitor sardine freshness and colour shifted from purple (fresh) to greenish purple (sub fresh) to completely green (spoiled). According to another study of Boonsiriwit et al. [75], pH freshness films based on hydroxypropyl methylcellulose/microcrystalline cellulose and butterfly pea anthocyanin changed colour from light purple to violet and finally green during mackerel spoilage.

The colour change of the smart labels was also quantified through total colour difference (ΔE) and the a-value difference (Δa), both of which consistently exceeded 3 (the lowest threshold detectable by the human eye) and progressively increased with the increasing spoilage rate of fish. ΔE and Δa were consistently higher under variable storage conditions than constant ones (Figure 17). By the end of the shelf life of the gilthead sea bream fillets, ΔE and Δa were 23.5 and 20.9 at constant and 35.7 and 33.0 at variable temperature conditions, respectively. Previous studies about smart films comprising anthocyanins and monitoring the freshness of various fish species have reported ΔE values around 48 after 9 days of storage at 4°C [75] or 57 after 3 days of storage at room temperature [76].

By correlating the measured microbial growth of the fish fillets (Figure 15) with the smart labels colour change at each time interval (Figure 17), it is possible to classify the freshness states of the fish and provide a discreet characterization for each one of them. As presented in Figure 18, there are 3 zones—fresh, moderate and spoilt—in which the fish could be classified depending on their freshness level. Specifically, the first freshness state included 'fresh' until the fourth and second day of fish storage at 1.7°C and variable temperature, respectively: < 5.5 log cfu/g and the colour of the smart labels gradually turned to light pink. The

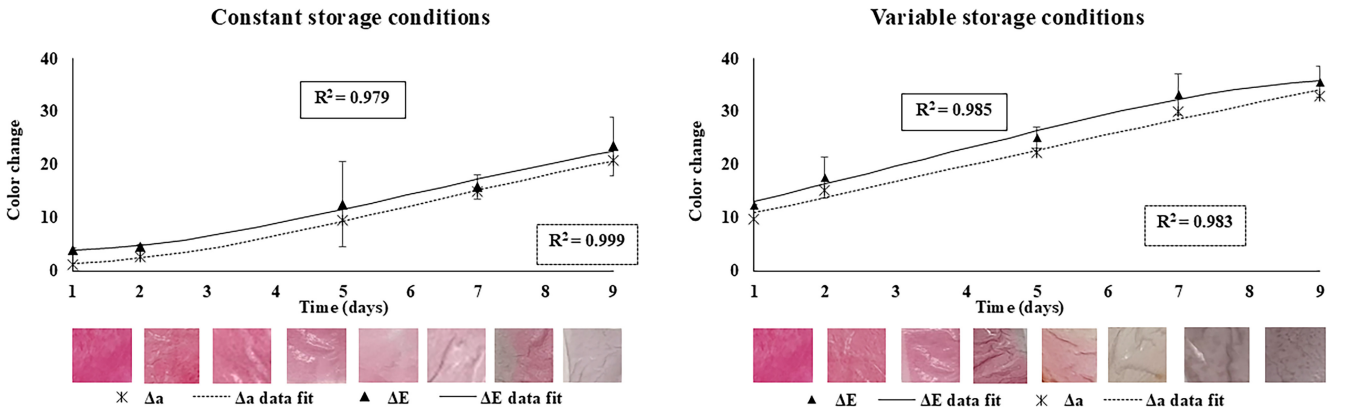

FIGURE 17 | Total colour difference (ΔE) and change in colour parameter a, Δa (a_0−a) of smart labels during storage at constant (1.7°C) and variable temperature conditions of sea bream fillets.

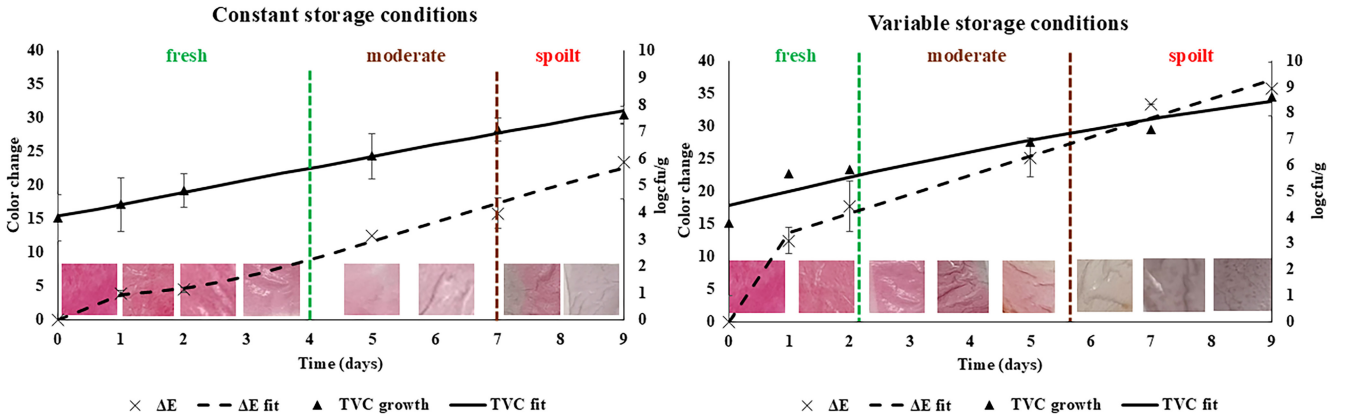

FIGURE 18 | Correlation of the colour change (ΔE) kinetics of the smart labels and the TVC growth kinetics during storage at constant (1.7°C) and variable temperature conditions of sea bream fillets.

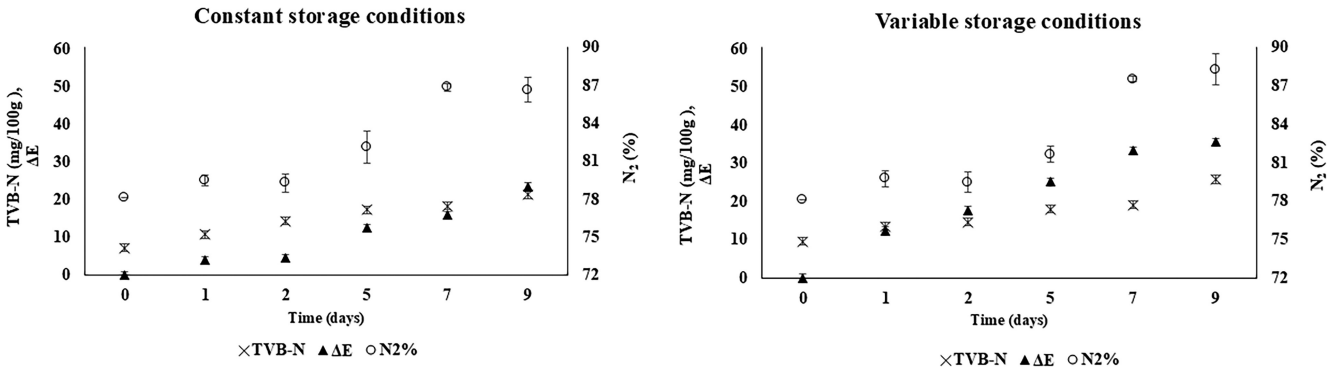

FIGURE 19 | Schematic presentation of TVB-N, colour change (ΔE) of the smart labels and in-package nitrogen concentration (N_2 %) during storage at constant (1.7°C) and variable temperature conditions of sea bream fillets.

second freshness state included 'moderate' until seventh and fifth day of fish storage at 1.7°C and variable temperature, respectively: < 7 log cfu/g and the colour of the smart labels gradually turned to colourless. Finally, the characterization 'spoilt' was given after 7 and 6 days of fish storage at 1.7°C and variable temperature, respectively: > 7 log cfu/g and the colour of the smart labels gradually turned to light green.

As shown in Figure 19, TVB-N progressed during fish storage experiments in a pattern similar to the smart labels' colour change (ΔE). A similar trend was observed in the in-package nitrogen (N_2%) concentration, indicating the ability of the smart labels to monitor fish freshness and highlight the impact of variable storage conditions during cold chain management.

Overall, the fabricated smart labels based on PVA/starch/anthocyanins demonstrated satisfactory performance in monitoring the freshness of gilthead sea bream fillets stored at constant (1.7°C) and variable temperature conditions. The colour change of the labels reflected the deterioration of fish quality in both storage scenarios, indicating their ability to signal fish spoilage due to temperature fluctuations during distribution and storage.

4 | Conclusion

Smart labels were produced from PVA and starch by incorporating anthocyanins derived from winery grape pomace. The grape pomace extract was rich in anthocyanins and exhibited sufficient pH sensitivity. Both control and smart films demonstrated satisfactory structural integrity, light barrier properties and water contact properties. The infusion of anthocyanins into the polymer matrix was successful, and the smart labels displayed increased sensitivity to a wide range of pH and volatile amines. The 45-day storage experiment indicated that temperature and RH significantly affected the properties of the films. At higher temperatures, the colour stability of the films weakened with increasing RH. The storage duration did not appear to significantly impact the wettability of the films, as similar results were observed at all time intervals. The intermediate storage temperature of 15°C appeared to favour both the water contact properties and colour stability of the films. During the fish freshness monitoring test, the smart labels effectively reflected the deterioration of fish quality in both constant and variable scenarios, exhibiting distinct visual colour changes (ΔE). Future research will focus on investigating further the rigidness and structure integrity of the smart films under different storage conditions to address limitations such as scalability.

Author Contributions

The study was designed by E.B. and T.T. The experiments were carried out by E.B. and E.M. and they were supervised by A.P. and T.T. The data analysis was carried out by E.B. and T.T. supervised the research. E.B., F.B., A.Q. and T.T. conceptualized the goals and aims of the research. E.B. wrote the main manuscript that was edited, completed, and reviewed by E.M., F.B., A.Q., A.P. and T.T.

Acknowledgements

The research work was supported by the Hellenic Foundation for Research and Innovation (HFRI) under the 5th Call for HFRI PhD Fellowships (Fellowship Number: 20599). This research has received partial funding from the European Union's Horizon 2020 research and innovation programme under the Marie Skłodowska-Curie Grant Agreement Number 872217 (ICHTHYS) (https://www.ichthys-eu.org/about).

Ethics Statement

The authors have nothing to report.

Conflicts of Interest

The authors declare no conflicts of interest.

Data Availability Statement

The data that support the findings of this study are available from the corresponding author upon reasonable request.

References

1. L. Skaf, P. P. Franzese, R. Capone, and E. Buonocore, "Unfolding Hidden Environmental Impacts of Food Waste: An Assessment for Fifteen Countries of the World," *Journal of Cleaner Production* 310 (2021): 127523, https://doi.org/10.1016/j.jclepro.2021.127523.

2. S. Mokrane, E. Buonocore, R. Capone, and P. P. Franzese, "Exploring the Global Scientific Literature on Food Waste and Loss," *Sustainability* 15, no. 6 (2023): 4757, https://doi.org/10.3390/su15064757.

3. D. Coppola, C. Lauritano, F. Palma Esposito, G. Riccio, C. Rizzo, and D. De Pascale, "Fish Waste: From Problem to Valuable Resource," *Marine Drugs* 19, no. 2 (2021): 116, https://doi.org/10.3390/md19020116.

4. Q. D. Read, S. Brown, A. D. Cuéllar, et al., "Assessing the Environmental Impacts of Halving Food Loss and Waste Along the Food Supply Chain," *Science of the Total Environment* 712 (2020): 136255, https://doi.org/10.1016/j.scitotenv.2019.136255.

5. T. N. Tsironi and P. S. Taoukis, "Current Practice and Innovations in Fish Packaging," *Journal of Aquatic Food Product Technology* 27, no. 10 (2018): 1024–1047, https://doi.org/10.1080/10498850.2018.1532479.

6. R. Abedi-Firoozjah, S. A. Salim, S. Hasanvand, et al., "Application of Smart Packaging for Seafood: A Comprehensive Review," *Comprehensive Reviews in Food Science and Food Safety* 22, no. 2 (2023): 1438–1461, https://doi.org/10.1111/1541-4337.13117.

7. X. Xiong, Y. Tan, E. Mubango, et al., "Rapid Freshness and Survival Monitoring Biosensors of Fish: Progress, Challenge, and Future Perspective," *Trends in Food Science & Technology* 129 (2022): 61–73, https://doi.org/10.1016/j.tifs.2022.08.011.

8. W. Wang, J. Liang, Y. Wu, et al., "Fish Freshness Monitoring Based on Bilayer Cellulose Acetate/Polyvinylidene Fluoride Membranes Containing ZIF-8 Loaded Curcumin," *Food Chemistry* 463 (2025): 141054, https://doi.org/10.1016/j.foodchem.2024.141054.

9. S. Chhikara and D. Kumar, "Edible Coating and Edible Film as Food Packaging Material: A Review," *Journal of Packaging Technology and Research* 6, no. 1 (2022): 1–10, https://doi.org/10.1007/s41783-021-00129-w.

10. "Regulation (EU) 2025/40 of the European Parliament and of the Council of 19 December 2024 on Packaging and Packaging Waste, Amending Regulation (EU) 2019/1020 and Directive (EU) 2019/904, and Repealing Directive 94/62/EC (Text With EEA Relevance)."

11. E. Basdeki, E. Mpenetou, P. Papazoglou, et al., "Evaluation of a Calcium Carbonate-Based Container for Transportation and Storage of Fresh Fish as a Sustainable Alternative to Polystyrene Boxes," *Sustainability* 16, no. 1 (2023): 130, https://doi.org/10.3390/su16010130.

12. M. Asgher, S. A. Qamar, M. Bilal, and H. M. N. Iqbal, "Bio-Based Active Food Packaging Materials: Sustainable Alternative to Conventional Petrochemical-Based Packaging Materials," *Food Research International* 137 (2020): 109625, https://doi.org/10.1016/j.foodres.2020.109625.

13. E. Athanasopoulou, A. Katsiroumpa, C. Gardeli, and T. Tsironi, "Comparative Study of Packaging Materials Developed From Fish and Legume Protein Concentrates," *Future Foods* 11 (2025): 100563, https://doi.org/10.1016/j.fufo.2025.100563.

14. A. Niponsak, N. Laohakunjit, O. Kerdchoechuen, P. Wongsawadee, and A. Uthairatanakij, "Novel Ripeness Label Based on Starch/Chitosan Incorporated With pH Dye for Indicating Eating Quality of Fresh–Cut Durian," *Food Control* 107 (2020): 106785, https://doi.org/10.1016/j.foodcont.2019.106785.

15. S. Patil, A. K. Bharimalla, A. Mahapatra, et al., "Effect of Polymer Blending on Mechanical and Barrier Properties of Starch-Polyvinyl Alcohol Based Biodegradable Composite Films," *Food Bioscience* 44 (2021): 101352, https://doi.org/10.1016/j.fbio.2021.101352.

16. S. I. R. Okoduwa, L. O. Mbora, M. E. Adu, and A. A. Adeyi, "Comparative Analysis of the Properties of Acid-Base Indicator of Rose (*Rosa setigera*), Allamanda (*Allamanda cathartica*), and Hibiscus (*Hibiscus rosa-sinensis*) Flowers," *Biochemistry Research International* 2015 (2015): 1–6, https://doi.org/10.1155/2015/381721.

17. J. Kan, J. Liu, F. Xu, D. Yun, H. Yong, and J. Liu, "Development of Pork and Shrimp Freshness Monitoring Labels Based on Starch/Polyvinyl Alcohol Matrices and Anthocyanins From 14 Plants: A Comparative Study," *Food Hydrocolloids* 124 (2022): 107293, https://doi.org/10.1016/j.foodhyd.2021.107293.

18. Q. Ma, L. Du, and L. Wang, "Tara Gum/Polyvinyl Alcohol-Based Colorimetric NH3 Indicator Films Incorporating Curcumin for Intelligent Packaging," *Sensors and Actuators B: Chemical* 244 (2017): 759–766, https://doi.org/10.1016/j.snb.2017.01.035.

19. X. Zhai, J. Shi, X. Zou, et al., "Novel Colorimetric Films Based on Starch/Polyvinyl Alcohol Incorporated With Roselle Anthocyanins for Fish Freshness Monitoring," *Food Hydrocolloids* 69 (2017): 308–317, https://doi.org/10.1016/j.foodhyd.2017.02.014.

20. B. Liu, H. Xu, H. Zhao, W. Liu, L. Zhao, and Y. Li, "Preparation and Characterization of Intelligent Starch/PVA Films for Simultaneous Colorimetric Indication and Antimicrobial Activity for Food Packaging Applications," *Carbohydrate Polymers* 157 (2017): 842–849, https://doi.org/10.1016/j.carbpol.2016.10.067.

21. M. H. Wathon, N. Beaumont, M. Benohoud, R. S. Blackburn, and C. M. Rayner, "Extraction of Anthocyanins From *Aronia melanocarpa* Skin Waste as a Sustainable Source of Natural Colorants," *Coloration Technology* 135, no. 1 (2019): 5–16, https://doi.org/10.1111/cote.12385.

22. O. Mileti, N. Baldino, F. Filice, F. R. Lupi, M. S. Sinicropi, and D. Gabriele, "Formulation Study on Edible Film From Waste Grape and Red Cabbage," *Food* 12, no. 14 (2023): 2804, https://doi.org/10.3390/foods12142804.

23. K. Ko, Y. Dadmohammadi, and A. Abbaspourrad, "Nutritional and Bioactive Components of Pomegranate Waste Used in Food and Cosmetic Applications: A Review," *Food* 10, no. 3 (2021): 657, https://doi.org/10.3390/foods10030657.

24. Z. Yu, V. Boyarkina, Z. Liao, M. Lin, W. Zeng, and X. Lu, "Boosting Food System Sustainability Through Intelligent Packaging: Application of Biodegradable Freshness Indicators," *ACS Food Science & Technology* 3, no. 1 (2023): 199–212, https://doi.org/10.1021/acsfoodscitech.2c00372.

25. C. Guo, Y. Li, H. Zhang, et al., "A Review on Improving the Sensitivity and Color Stability of Naturally Sourced pH-Sensitive Indicator Films," *Comprehensive Reviews in Food Science and Food Safety* 23, no. 4 (2024): e13390, https://doi.org/10.1111/1541-4337.13390.

26. I. Chiu and T. Yang, "Biopolymer-Based Intelligent Packaging Integrated With Natural Colourimetric Sensors for Food Safety and Sustainability," *Analytical Science Advances* 5, no. 5–6 (2024): e2300065, https://doi.org/10.1002/ansa.202300065.

27. O. Romruen, P. Kaewprachu, S. Sai-Ut, et al., "Impact of Environmental Storage Conditions on Properties and Stability of a Smart Bilayer Film," *Scientific Reports* 14, no. 1 (2024): 23038, https://doi.org/10.1038/s41598-024-74004-4.

28. M. Alizadeh Sani, M. Tavassoli, S. A. Salim, M. Azizi-lalabadi, and D. J. McClements, "Development of Green Halochromic Smart and Active Packaging Materials: TiO_2 Nanoparticle- and Anthocyanin-Loaded Gelatin/κ-Carrageenan Films," *Food Hydrocolloids* 124 (2022): 107324, https://doi.org/10.1016/j.foodhyd.2021.107324.

29. Y. Qin, D. Yun, F. Xu, D. Chen, J. Kan, and J. Liu, "Smart Packaging Films Based on Starch/Polyvinyl Alcohol and *Lycium ruthenicum* Anthocyanins-Loaded Nano-Complexes: Functionality, Stability and Application," *Food Hydrocolloids* 119 (2021): 106850, https://doi.org/10.1016/j.foodhyd.2021.106850.

30. Y. Qin, Y. Liu, H. Yong, J. Liu, X. Zhang, and J. Liu, "Preparation and Characterization of Active and Intelligent Packaging Films Based on Cassava Starch and Anthocyanins From *Lycium ruthenicum* Murr," *International Journal of Biological Macromolecules* 134 (2019): 80–90, https://doi.org/10.1016/j.ijbiomac.2019.05.029.

31. A. P. Kondratov, A. A. Volinsky, and J. Chen, "Scaling Effects on Color and Transparency of Multilayer Polyethylene Films in Polarized Light," *Advances in Polymer Technology* 37, no. 3 (2018): 668–673, https://doi.org/10.1002/adv.21708.

32. L. Jia, W. Sun, W. Li, et al., "A Colour Indicator Film Based on Bromothymol Blue/Poly-L-Lactic Acid/Polyvinylpyrrolidone for Detecting

Bacteria," *Packaging Technology and Science* 36, no. 7 (2023): 549–556, https://doi.org/10.1002/pts.2726.

33. B. Kuswandi, A. Restyana, A. Abdullah, L. Y. Heng, and M. Ahmad, "A Novel Colorimetric Food Package Label for Fish Spoilage Based on Polyaniline Film," *Food Control* 25, no. 1 (2012): 184–189, https://doi.org/10.1016/j.foodcont.2011.10.008.

34. G. Oliveira, I. Gonçalves, A. Barra, C. Nunes, P. Ferreira, and M. A. Coimbra, "Coffee Silverskin and Starch-Rich Potato Washing Slurries as Raw Materials for Elastic, Antioxidant, and UV-Protective Biobased Films," *Food Research International* 138 (2020): 109733, https://doi.org/10.1016/j.foodres.2020.109733.

35. Y. Yuan and T. R. Lee, "Contact Angle and Wetting Properties," in *Surface Science Techniques. Vol 51. Springer Series in Surface Sciences*, eds. G. Bracco and B. Holst (Springer Berlin Heidelberg, 2013), 3–34, https://doi.org/10.1007/978-3-642-34243-1_1.

36. R. Ran, S. Chen, Y. Su, et al., "Preparation of pH-Colorimetric Films Based on Soy Protein Isolate/ZnO Nanoparticles and Grape-Skin Red for Monitoring Pork Freshness," *Food Control* 137 (2022): 108958, https://doi.org/10.1016/j.foodcont.2022.108958.

37. J. Blahovec and S. Yanniotis, "GAB Generalized Equation for Sorption Phenomena," *Food and Bioprocess Technology* 1, no. 1 (2008): 82–90, https://doi.org/10.1007/s11947-007-0012-3.

38. B. Fu and T. P. Labuza, "Shelf-Life Testing: Procedures and Prediction Methods," in *Quality in Frozen Foods*, eds. M. C. Erickson and Y. C. Hung (Springer US, 1997), 377–415, https://doi.org/10.1007/978-1-4615-5975-7_19.

39. K. Koutsoumanis, "Predictive Modeling of the Shelf Life of Fish Under Nonisothermal Conditions," *Applied and Environmental Microbiology* 67, no. 4 (2001): 1821–1829, https://doi.org/10.1128/AEM.67.4.1821-1829.2001.

40. K. C. A. Garber, A. Y. Odendaal, and E. E. Carlson, "Plant Pigment Identification: A Classroom and Outreach Activity," *Journal of Chemical Education* 90, no. 6 (2013): 755–759, https://doi.org/10.1021/ed200823t.

41. C. L. Luchese, V. F. Abdalla, J. C. Spada, and I. C. Tessaro, "Evaluation of Blueberry Residue Incorporated Cassava Starch Film as pH Indicator in Different Simulants and Foodstuffs," *Food Hydrocolloids* 82 (2018): 209–218, https://doi.org/10.1016/j.foodhyd.2018.04.010.

42. M. Lakshmikanthan, S. Muthu, K. Krishnan, et al., "A Comprehensive Review on Anthocyanin-Rich Foods: Insights Into Extraction, Medicinal Potential, and Sustainable Applications," *Journal of Agriculture and Food Research* 17 (2024): 101245, https://doi.org/10.1016/j.jafr.2024.101245.

43. C. A. Gómez-Aldapa, G. Velazquez, M. C. Gutierrez, E. Rangel-Vargas, J. Castro-Rosas, and R. Y. Aguirre-Loredo, "Effect of Polyvinyl Alcohol on the Physicochemical Properties of Biodegradable Starch Films," *Materials Chemistry and Physics* 239 (2020): 122027, https://doi.org/10.1016/j.matchemphys.2019.122027.

44. S. Wang, P. Xia, S. Wang, et al., "Packaging Films Formulated With Gelatin and Anthocyanins Nanocomplexes: Physical Properties, Antioxidant Activity and Its Application for Olive Oil Protection," *Food Hydrocolloids* 96 (2019): 617–624, https://doi.org/10.1016/j.foodhyd.2019.06.004.

45. M. Chandra Singh, W. E. Price, C. Kelso, K. Charlton, and Y. Probst, "Impact of Molar Absorbance on Anthocyanin Content of the Foods," *Food Chemistry* 386 (2022): 132855, https://doi.org/10.1016/j.foodchem.2022.132855.

46. M. Koosha and S. Hamedi, "Intelligent Chitosan/PVA Nanocomposite Films Containing Black Carrot Anthocyanin and Bentonite Nanoclays With Improved Mechanical, Thermal and Antibacterial Properties," *Progress in Organic Coatings* 127 (2019): 338–347, https://doi.org/10.1016/j.porgcoat.2018.11.028.

47. H. Hu, J. Chen, C. Lin, H. Sun, and Y. Chen, "Characterization of Edible pH-Responsive Ink Based on Carboxymethyl Chitosan and Purple Potato Anthocyanin/Curcumin for Monitoring Pork Freshness," *Packaging Technology and Science* 38 (2024): pts.2867, https://doi.org/10.1002/pts.2867.

48. F. Moeinpour and F. S. Mohseni-Shahri, "Properties of Roselle and Alizarin Mixed Loaded Gelatin Films as a pH-Sensing Indicator for Shrimp Freshness Monitoring," *Packaging Technology and Science* 36, no. 6 (2023): 483–493, https://doi.org/10.1002/pts.2724.

49. G. Esposito, S. Sciuto, and P. L. Acutis, "Quantification of TMA in Fishery Products by Direct Sample Analysis With High Resolution Mass Spectrometry," *Food Control* 94 (2018): 162–166, https://doi.org/10.1016/j.foodcont.2018.07.010.

50. P. C. Ellis, L. F. Pivarnik, M. Thiam, and Collaborators: Berger L Field S Green D Hewes D Lemerise D Lyttle C Maciel J Soper K, "Determination of Volatile Bases in Seafood Using the Ammonia Ion Selective Electrode: Collaborative Study," *Journal of AOAC International* 83, no. 4 (2000): 933–943, https://doi.org/10.1093/jaoac/83.4.933.

51. M. Ameri, A. Ajji, and S. Kessler, "Characterization of a Food-Safe Colorimetric Indicator Based on Black Rice Anthocyanin/PET Films for Visual Analysis of Fish Spoilage," *Packaging Technology and Science* 37, no. 8 (2024): 769–780, https://doi.org/10.1002/pts.2824.

52. H. Tian, J. Yan, A. V. Rajulu, A. Xiang, and X. Luo, "Fabrication and Properties of Polyvinyl Alcohol/Starch Blend Films: Effect of Composition and Humidity," *International Journal of Biological Macromolecules* 96 (2017): 518–523, https://doi.org/10.1016/j.ijbiomac.2016.12.067.

53. C. Wang and C. Liu, "A pH-Sensitive Intelligent Packaging Film Harnessing Anthocyanin for Food Freshness Monitoring," *Food and Bioprocess Technology* 17, no. 12 (2024): 5312–5323, https://doi.org/10.1007/s11947-024-03431-y.

54. V. A. Pereira, I. N. Q. De Arruda, and R. Stefani, "Active Chitosan/PVA Films With Anthocyanins From *Brassica oleraceae* (Red Cabbage) as Time–Temperature Indicators for Application in Intelligent Food Packaging," *Food Hydrocolloids* 43 (2015): 180–188, https://doi.org/10.1016/j.foodhyd.2014.05.014.

55. Y. Zheng, X. Li, Y. Huang, H. Li, L. Chen, and X. Liu, "Two Colorimetric Films Based on Chitin Whiskers and Sodium Alginate/Gelatin Incorporated With Anthocyanins for Monitoring Food Freshness," *Food Hydrocolloids* 127 (2022): 107517, https://doi.org/10.1016/j.foodhyd.2022.107517.

56. E. Fathi, N. Atyabi, M. Imani, and Z. Alinejad, "Physically Crosslinked Polyvinyl Alcohol–Dextran Blend Xerogels: Morphology and Thermal Behavior," *Carbohydrate Polymers* 84, no. 1 (2011): 145–152, https://doi.org/10.1016/j.carbpol.2010.11.018.

57. M. Işılay, A. Çay, Ç. Akduman, E. P. A. Kumbasar, and H. Ertaş, "Morphology and Methanol Permeability of Sulfosuccinic Acid Cross-Linked Polyvinyl Alcohol and Polyvinyl Alcohol/Nafion Nanofibrous Membranes," *Journal of Applied Polymer Science* 142, no. 2 (2025): e56346, https://doi.org/10.1002/app.56346.

58. S. Roy and J. W. Rhim, "Anthocyanin Food Colorant and Its Application in pH-Responsive Color Change Indicator Films," *Critical Reviews in Food Science and Nutrition* 61, no. 14 (2021): 2297–2325, https://doi.org/10.1080/10408398.2020.1776211.

59. H. Yong and J. Liu, "Recent Advances in the Preparation, Physical and Functional Properties, and Applications of Anthocyanins-Based Active and Intelligent Packaging Films," *Food Packaging and Shelf Life* 26 (2020): 100550, https://doi.org/10.1016/j.fpsl.2020.100550.

60. A. Jayakumar, S. Radoor, G. H. Shin, S. Siengchin, and J. T. Kim, "Active and Intelligent Packaging Films Based on PVA/Chitosan/Zinc Oxide Nanoparticles/Sweet Purple Potato Extract as pH Sensing and Antibacterial Wraps," *Food Bioscience* 56 (2023): 103432, https://doi.org/10.1016/j.fbio.2023.103432.

61. C. M. Willemse, M. A. Stander, and A. De Villiers, "Hydrophilic Interaction Chromatographic Analysis of Anthocyanins," *Journal of Chromatography A* 1319 (2013): 127–140, https://doi.org/10.1016/j.chroma.2013.10.045.

62. W. Lin, Y. Ni, and J. Pang, "Microfluidic Spinning of Poly (Methyl Methacrylate)/Konjac Glucomannan Active Food Packaging Films Based on Hydrophilic/Hydrophobic Strategy," *Carbohydrate Polymers* 222 (2019): 114986, https://doi.org/10.1016/j.carbpol.2019.114986.

63. W. Pan, Q. Liang, and Q. Gao, "Preparation of Hydroxypropyl Starch/Polyvinyl Alcohol Composite Nanofibers Films and Improvement of Hydrophobic Properties," *International Journal of Biological Macromolecules* 223 (2022): 1297–1307, https://doi.org/10.1016/j.ijbiomac.2022.11.114.

64. Q. Xiong, Q. Mo, X. Yue, et al., "A Smart Superwetting PET-Anthocyanin Membrane for pH Monitoring in Water and Emulsion Separation," *Journal of Industrial and Engineering Chemistry* 132 (2024): 507–517, https://doi.org/10.1016/j.jiec.2023.11.045.

65. A. P. Teodoro, S. Mali, N. Romero, and G. M. De Carvalho, "Cassava Starch Films Containing Acetylated Starch Nanoparticles as Reinforcement: Physical and Mechanical Characterization," *Carbohydrate Polymers* 126 (2015): 9–16, https://doi.org/10.1016/j.carbpol.2015.03.021.

66. H. A. Iglesias, R. Baeza, and J. Chirife, "A Survey of Temperature Effects on GAB Monolayer in Foods and Minimum Integral Entropies of Sorption: A Review," *Food and Bioprocess Technology* 15, no. 4 (2022): 717–733, https://doi.org/10.1007/s11947-021-02740-w.

67. C. M. P. Yoshida, V. B. V. Maciel, M. E. D. Mendonça, and T. T. Franco, "Chitosan Biobased and Intelligent Films: Monitoring pH Variations," *LWT - Food Science and Technology* 55, no. 1 (2014): 83–89, https://doi.org/10.1016/j.lwt.2013.09.015.

68. A. Sinela, N. Rawat, C. Mertz, N. Achir, H. Fulcrand, and M. Dornier, "Anthocyanins Degradation During Storage of Hibiscus Sabdariffa Extract and Evolution of Its Degradation Products," *Food Chemistry* 214 (2017): 234–241, https://doi.org/10.1016/j.foodchem.2016.07.071.

69. S. Kang, H. Wang, L. Xia, et al., "Colorimetric Film Based on Polyvinyl Alcohol/Okra Mucilage Polysaccharide Incorporated With Rose Anthocyanins for Shrimp Freshness Monitoring," *Carbohydrate Polymers* 229 (2020): 115402, https://doi.org/10.1016/j.carbpol.2019.115402.

70. T. Tsironi, A. Ntzimani, E. Gogou, et al., "Modeling the Effect of Active Modified Atmosphere Packaging on the Microbial Stability and Shelf Life of Gutted Sea Bass," *Applied Sciences* 9, no. 23 (2019): 5019, https://doi.org/10.3390/app9235019.

71. ICMSF, "Sampling Plans for Fish and Shellfish," in *Microorganisms in Food 2: Sampling for Microbiological Analysis: Principles and Specific Applications*, 2nd ed. (Blackwell Scientific Publications, 1986).

72. E. Basdeki, S. E. Vasilaki, M. Sensi, et al., "Reviewing the Correlation of Fish Quality Alteration and In-Package Headspace Composition: Evidence From a pH Freshness Indicator Case Study," *International Journal of Food Science* 2025, no. 1 (2025): 3576183, https://doi.org/10.1155/ijfo/3576183.

73. M. Jakobsen and G. Bertelsen, "The Use of CO_2 in Packaging of Fresh Red Meats and Its Effect on Chemical Quality Changes in the Meat: A Review," *Journal of Muscle Foods* 13, no. 2 (2002): 143–168, https://doi.org/10.1111/j.1745-4573.2002.tb00326.x.

74. R. R. Koshy, K. Vishnu, A. Reghunadhan, et al., "Biofilms From Poly-Vinyl Alcohol/Palmyra Root Sprout With *Boswellia serrata*, Carbon Dots and Anthocyanin for Sensing the Freshness of Sardine Fish," *International Journal of Biological Macromolecules* 273 (2024): 132991, https://doi.org/10.1016/j.ijbiomac.2024.132991.

75. A. Boonsiriwit, M. Lee, M. Kim, P. Inthamat, U. Siripatrawan, and Y. S. Lee, "Hydroxypropyl Methylcellulose/Microcrystalline Cellulose Biocomposite Film Incorporated With Butterfly Pea Anthocyanin as a Sustainable pH-Responsive Indicator for Intelligent Food-Packaging Applications," *Food Bioscience* 44 (2021): 101392, https://doi.org/10.1016/j.fbio.2021.101392.

76. M. Tavassoli, A. Khezerlou, M. Bakhshizadeh, et al., "Smart Packaging Containing Red Poppy Anthocyanins for Fish Freshness Monitoring," *Journal of Food Measurement and Characterization* 18, no. 4 (2024): 3054–3068, https://doi.org/10.1007/s11694-024-02386-0.